FEASIBILITY OF USING NONLINEAR TIME-FREQUENCY CONTROL FOR MAGNETORHEOLOGICAL DAMPERS IN VEHICLE SUSPENSION

A Thesis

by

EVAN DALTON WRIGHT

Submitted to the Office of Graduate and Professional Studies of
Texas A&M University
in partial fulfillment of the requirements for the degree of

MASTER OF SCIENCE

Chair of Committee,	C. Steve Suh
Committee Members,	Stefan Hurlebaus
	Sai Lau
Head of Department,	Andreas Polycarpou

May 2017

Major Subject: Mechanical Engineering

Copyright 2017 Evan Wright

ABSTRACT

Semi-active vehicle suspensions that use magnetorheological (MR) dampers are able to better dissipate vibrations compared to conventional dampers because of their controllable damping characteristics. The performance of current MR damper control methods is often hindered by incorrect assumptions and linearized models. Therefore, a need exists to design an adaptive controller with improved accuracy and reliability. The objective of this research is to design an improved controller for MR dampers in vehicle suspension using the nonlinear time-frequency control approach and evaluate its feasibility by numerically employing MATLAB Simulink. Simulations in this research are performed using a simplified quarter car suspension model and modified Bouc-Wen damper model. The proposed control method is evaluated based on its ability to reduce the amplitude of vibrations and minimize acceleration of the car body for various test cases. Simulations are also performed using the skyhook controller and passive suspension to assess the performance of the proposed controller.

The results of the simulations show that the proposed nonlinear time-frequency controller can successfully be applied to an MR damper suspensions system for vibration control. The proposed controller outperforms the skyhook controller in terms of reducing acceleration of the car body in each of the tested scenarios. The proposed controller also shows the ability to more efficiently manage the current input to the system. In general, the skyhook controller gives more improved vibration amplitude responses but is prone to generate large spikes in car body acceleration at higher frequency road profile inputs.

Simulations performed with the passive system show large displacement amplitudes and inability to prevent oscillation. The feed-forward aspect and adaptive nature of the proposed controller gives it the ability to better compensate for the time-delay in the operation of the MR damper. The proposed controller shows sensitivity to controller parameters when pursuing the best response for different road profile input cases.

CONTRIBUTORS AND FUNDING SOURCES

This work was supervised by a thesis committee consisting of Professors C. Steve Suh and Sai Lau of the Department of Mechanical Engineering and Professor Stefan Hurlebaus of the Department of Civil Engineering.

All work for the thesis was completed by the student, under the advisement of C. Steve Suh of the Department of Mechanical Engineering.

There are no outside funding contributions to acknowledge related to the research and compilation of this document.

TABLE OF CONTENTS

Page

LIST OF FIGURES

Page

LIST OF TABLES

Page

1. INTRODUCTION

1.1 Magnetorheological Dampers

Magnetorheological (MR) dampers are the leading technology in high performance vehicle suspensions. They can be found in several makes of vehicles including Cadillac, Chevrolet, Acura, Ferrari, and Audi. Vehicle suspensions are evaluated by how well they reduce road vibrations, minimize forces experienced by the passengers and how they improve the handling and stability of the vehicle. Suspensions that use MR dampers are referred to as semi-active because the damping forces can be controlled depending on the conditions the vehicle is subject to, but still retain damping ability should the control system fail. Semi-active suspensions provide great benefits in terms of vehicle response over a broader range of frequencies compared to conventional vehicle suspensions.

To better explain the concept of a semi-active control, examples of force versus velocity plots are provided in Figure 1 for passive, semi-active, and fully active systems [1]. The semi-active force region is referred to as its dissipative domain; hence why semi-active control is limited to cases where vibration energy can be dissipated. Consequently, traditional control strategies cannot always be used for MR damper systems. In contrast, the available control force for a fully active systems is independent of relative velocity because they are able to input additional energy into the system to provide control [1].

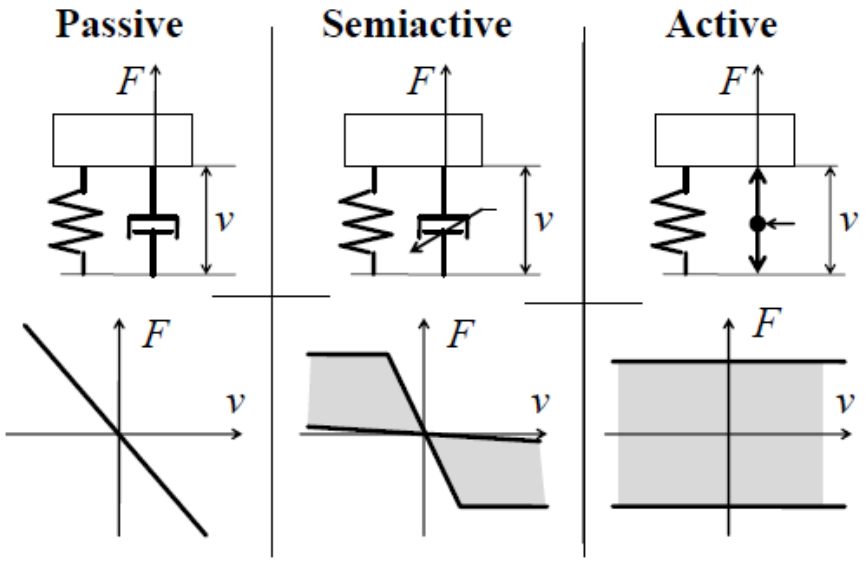

Figure 1: Force range characteristics of passive, semi-active and active systems [1]

MR dampers are characterized by containing magnetic particles (usually iron-nickel and iron-cobalt alloys) suspended in the working fluid of the damper cylinder. The viscosity of MR fluid can be altered by varying the current applied to the fluid and changing the magnetic field [2]. Upon exposure to a magnetic field, the magnetic particles in the fluid align along the magnetic lines of force (shown in Figure 2) [3]. The formed lines of magnetic particles require more force to be rearranged; effectively increasing the viscosity of the fluid.

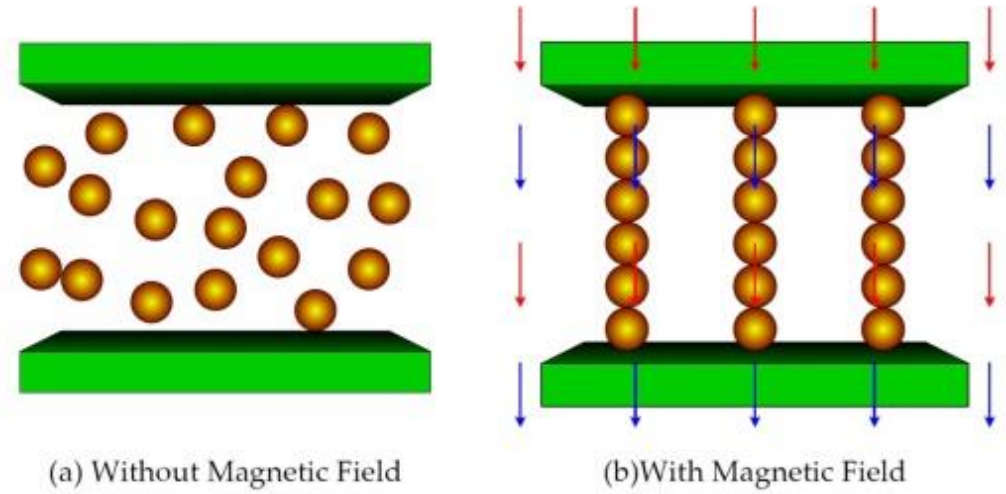

Figure 2: Illustrated effect of magnetic field [3]

A cross-sectional diagram showing the main components of the MR damper is given in Figure 3 [3]. There are multiple available methods that can be used to model the operation of MR dampers. Popular methods include Bingham, Dahl, Bouc-Wen, and Modified Bouc-Wen. The Modified Bouc-Wen model was chosen for the simulations performed in this research. This model and its corresponding equations are explained in Section 3.2.

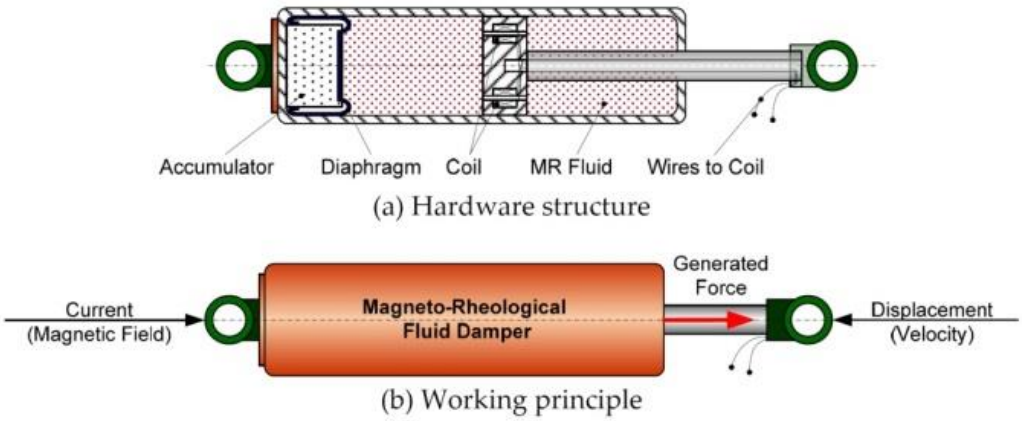

Figure 3: Diagram of MR Damper [3]

1.2 Commonly Used Semi-Active Control Strategies

Various methods that have shown to be capable of controlling MR dampers are described in this section. The performance of current MR damper control methods is often hindered by incorrect assumptions. For example, feedback techniques do not possess a way to account for the time-delay of the MR damper itself. Other methods lose accuracy by linearizing the equations that define the physical model.

1.2.1 Skyhook Control Algorithm

The skyhook control algorithm is widely used in semi-active vehicle suspension control due to its simplicity. The skyhook method requires sensors to measure sprung-mass acceleration and relative displacement. These two signals are then converted into the corresponding velocities which determine the required damping forces to reduce vibration. In more advanced skyhook control schemes, the control module receives sensor inputs from suspension height, throttle position, steering wheel position, and

wheel speed to counteract roll, pitch, and yaw of the vehicle. This more complicated configuration requires the damper control system to be completely integrated with the vehicle and ECU. [4] This presents challenges in implementing an aftermarket magnetic damper system and interfacing it to existing vehicle's system. The main drawback to a feedback algorithm such as skyhook is that it is not adaptive and cannot account for the delay in response time of the MR damper as well as a feedforward algorithm. [5] This disadvantage leads to a decrease in performance of skyhook control at high frequency vibrations; however in an actual vehicle model, high frequency vibrations are often dissipated by the wheel and tire and the car body experiences some degree of vibration isolation.

1.2.2 Optimal Control

Optimal control algorithms utilizing Linear-Quadratic Regulator (LQR) or Linear-Quadratic Gaussian (LQG) have been used in numerous control methods for MR dampers. The LQG controller employs a Kalman filter state estimator that is integrated in the controller. A major drawback to using the Kalman filter is that the equations for the system and observation model are assumed to be linear. [6] For a highly nonlinear case such as MR dampers, these assumptions are not realistic and can present possible issues concerning the accuracy of the controller. The LQR method faces shortcomings in its inability to account for excitation in the forced vibration of structures. To represent practical situations the excitation must be known beforehand to produce ideal control forces. Wavelet based LQR methods have shown to be more effective than conventional

LQR in terms of improving the displacement response of a structure in the time domain. [7] The clipped-optimal control algorithm proposed by Dyke *et al*. [8] is based on reducing either the acceleration or displacement of the structure for a given response. The method utilizes an optimal controller to identify a desired control force and a clipping algorithm to convert the desired force to voltage or current.

1.2.3 Fuzzy Logic Control

Fuzzy logic control is also often used in highly nonlinear semi-active systems. Fuzzy logic is advantageous to many other control techniques because it does not require a precise mathematical model to provide control. However, the design of a fuzzy logic controller often relies on trial and error or the designer's experience. [9] For a given system to function properly with a fuzzy controller, the fuzzy rules must be pre-determined. Genetic algorithms can be used to optimize the number of fuzzy rules and membership functions. The research presented by Yan and Zhou [10] uses genetic algorithms as an adaptive method to design the fuzzy controller.

1.2.4 Control Using Preview Signal Input

Other methods are able to take advantage of road preview information when equipped with the proper sensors. The preview signal is acquired using sensors that scan the road profile to determine the upcoming vertical displacement. This signal can then be used to calculate a desired damping force. The method presented by Krauze and Kasprzyk [5] uses this technology combined with a modified FXLMS algorithm to

control vibration in a vehicle. The disadvantage to this approach is that it cannot function without the additional scanning sensors. There is also a source of error in this method using the inverse MR damper model to convert the desired control force to voltage or current. Controllers that utilize an inverse MR damper model to calculate controlled voltage or current are linearized to some degree and therefore lose accuracy.

1.3 Applications of Nonlinear Time – Frequency Control

The concept of the nonlinear time-frequency control method presented in this research has been applied to several mechanical systems that operate using fully active control. The ideology behind this control method was explained by Suh and Liu [11] along with its applications in milling, micro-machining, and friction induced instability. A detailed description of this control scheme is presented in Section 2.3.

This control scheme has shown to be successful in controlling active magnetic bearings in a flywheel energy storage system by Lewallen [12]. Results of this research showed that the proposed controller provided reliable control at high operating speeds and stability in the frequency domain when external excitations are limited. Another application of this control scheme to active magnetic bearings was researched by Liu [13] for high speed spindle design. The simulations performed in this research showed reliable vibration control with regard for the gyroscopic effect and geometric coupling that other models disregard.

A modified version of this controller utilizing a time-varying reference signal was presented by Wang and Suh [14] for concurrent speed and precision tracking of a

brushed DC motor. The fundamental difference in this controller is that a proportional controller was implemented in the speed control scheme to compensate the time-delay of the on-line identification process. The results of this research showed this technique was able to provide accurate simultaneous position and speed control while reducing the power required by the motor compared to PID and Fuzzy Logic controllers.

The success of nonlinear time-frequency control in fully active control applications suggests that it may be able to provide improvement in a semi-active system as well. The fundamental difference in implementing this method in a semi-active system is that control forces cannot be directly manipulated. For the case of MR dampers, only the damping characteristics of the system can be controlled and control force is also a function of relative velocity between the wheel mass and car body mass.

1.4 Research Objective

Control methods currently available for MR dampers in vehicle suspension each come with their own imperfections and disadvantages. There is a need to design a controller with improved accuracy and reliability that is adaptive and does not rely on linearized models and unrealistic assumptions.

The objective of this research is to design an improved controller for MR dampers using the nonlinear time-frequency control approach and evaluate its feasibility when applied to vehicle suspensions. Simulations will be performed in MATLAB and Simulink using the selected vehicle model for various road conditions. Vehicle response using the proposed nonlinear time-frequency controller will be compared with results

from the skyhook controller and passive suspension. Performance of the controller will be assessed in terms of its ability to reduce the amplitude of vibrations and minimize the acceleration of the car body.

1.5 Research Task Plan

1. Develop Analytical Model:

Parameters will be defined for the suspension of a quarter car model of a light passenger vehicle. The Modified Bouc-Wen model will be used to characterize the properties of the MR damper.

2. Design Nonlinear Time-Frequency Controller for Model:

A wavelet based nonlinear time-frequency control scheme will be developed to control the MR damper in the quarter car model.

3. Formulate Test Cases:

The vehicle suspension model will be tested for road profile cases involving different types of vibration excitation and a single large bump.

4. Evaluate Controller by Comparison:

The results produced by the simulations using the proposed nonlinear time-frequency control scheme will be compared with the skyhook controller and

passive system for evaluation. Areas of interest are response time, vibration reduction, efficiency, and accuracy of the controller.

2. NONLINEAR TIME-FREQUENCY CONTROL CONCEPT

In this section, the proposed wavelet based time-frequency control concept to be applied to MR dampers is presented. This nonlinear control method relies on the principle defined by the Parseval's Theorem that energies computed in the time and frequency domains are interchangeable. Therefore, vibration amplitudes in the time domain and vibration spectra in the frequency domain need to be accounted for simultaneously. The time-frequency control method is adaptive, allowing for adjustments to be made to improve a system's performance. Wavelet coefficients are adjusted in the time domain to achieve simultaneous time-frequency control. The adaptive algorithm used in this controller is the filtered - X least mean square algorithm (FXLMS). A schematic of the controller configuration is presented in Figure 4 [11].

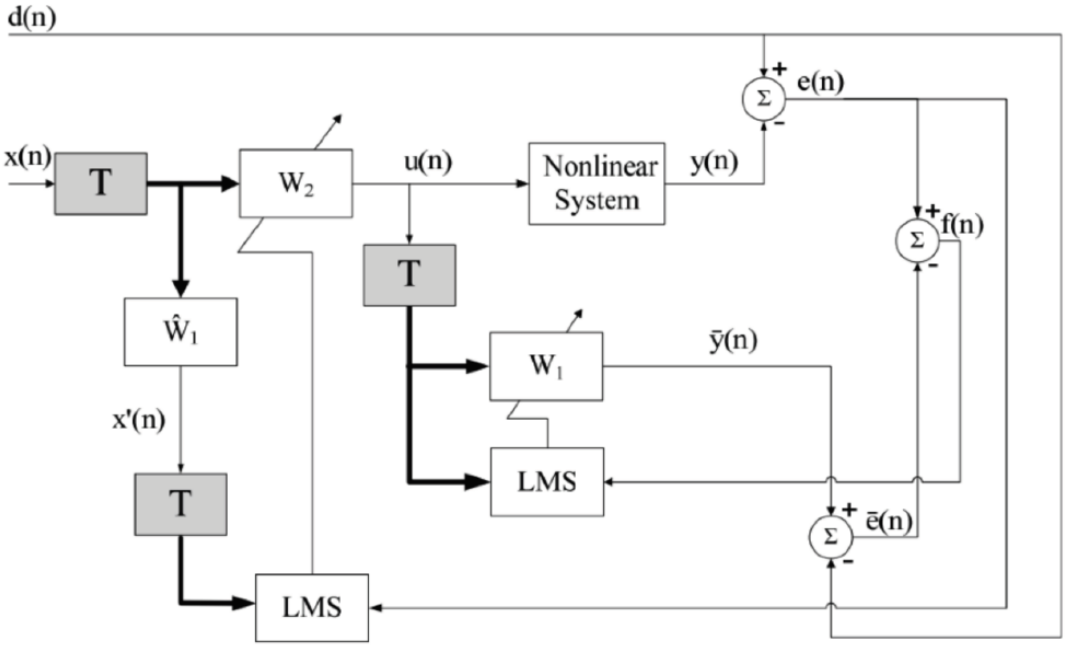

Figure 4: Wavelet based nonlinear time-frequency control [11]

The time-domain discrete signal *x(n)* is converted into a wavelet coefficient array by the $N \times N$ discrete wavelet transform matrix *T*. The wavelet coefficient array is then multiplied by the weights of the finite impulse response (FIR) filters, W_1 and W_2, and summed to reconstruct the time-domain signal. The first adaptive filter W_1 is used for system identification and models the system on-line. The second adaptive filter W_2 is used as the feed-forward controller. The weight vectors are given by Equations 1 and 2.

$$W_1(n) = [w_{1,0}(n), w_{1,1}(n), \dots, w_{1,N-1}(n)] \quad [1]$$

$$W_2(n) = [w_{2,0}(n), w_{2,1}(n), \dots, w_{2,N-1}(n)] \quad [2]$$

Equation 3 gives the identification error, $\bar{e}(n)$, between the desired signal $d(n)$ and the output from W_1. Where $\bar{y}(n)$ is defined by Equation 4.

$$\bar{e}(n) = d(n) - \bar{y}(n) \quad [3]$$

$$\bar{y}(n) = W_1^T(n)\, T\, U(n) \quad [4]$$

The error between the physical system and the desired signal is calculated by Equation 5.

$$e(n) = d(n) - y(n) \quad [5]$$

The identification error, $f(n)$, is then used to optimize the coefficients of the adaptive filter W_1.

$$f(n) = e(n) - \bar{e}(n) \quad [6]$$

The adaptive algorithms that are used to update the weights of the filters W_1 and W_2 are given by Equations 7 and 8. The variables μ_1 and μ_2 are the optimization step sizes used to minimize the error in the LMS regression scheme. The term x', defined by Equation 9, is the output of the filter $\widehat{W_1}$. This filter is used to compensate for possible disturbances in the propagation route of $u(n)$ [14].

$$W_1(n+1) = W_1(n) - \mu_1\, T\, U(n)\, f(n) \quad [7]$$

$$W_2(n+1) = W_2(n) + \mu_2\, T\, X'(n)\, e(n)) \quad [8]$$

$$x'(n) = W_1^T\, T\, X(n) \quad [9]$$

The controller parameters that must be specified in the programming include the initial values for the filters W_1 and W_2, the wavelet filter length N, the regression step sizes μ_1 and μ_2 and the time step. These values will be presented with the results.

The discrete wavelet transform matrix T used to decompose the input signal into wavelet coefficients is created using the Daubechies-3 (DB3) wavelet. Plots of the DB3 wavelet and scaling functions are shown in Figure 5. The coefficients used to construct the DB3 wavelet are given in Table 1.

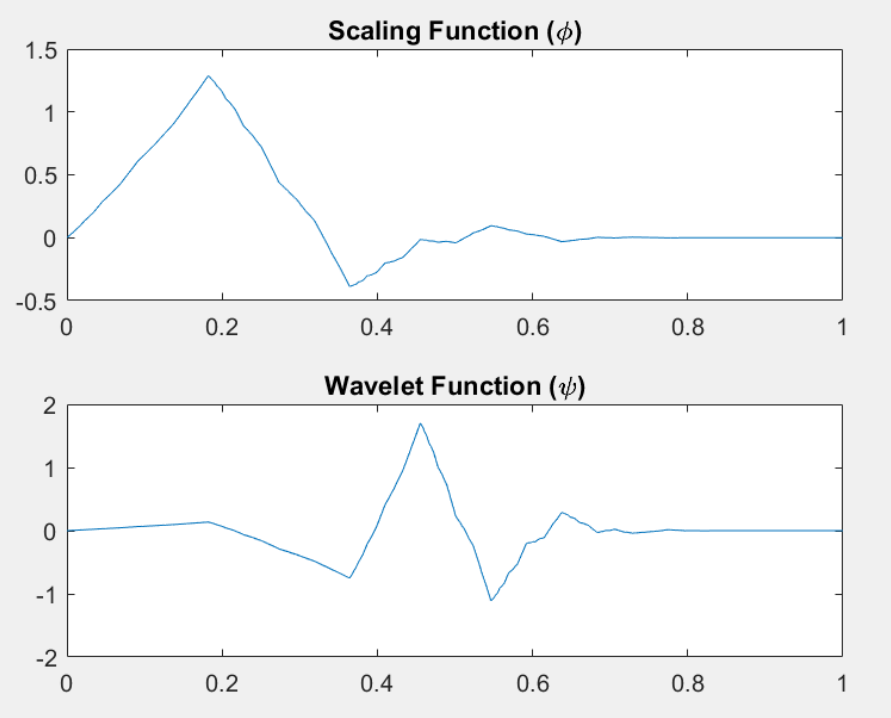

Figure 5: DB3 Wavelet

Table 1: DB3 high-pass & low-pass filter coefficients

$h_1 = 0.33267055295095688$	$g_1 = h_6$
$h_2 = 0.80689150931333875$	$g_2 = -h_5$
$h_3 = 0.45987750211933132$	$g_3 = h_4$
$h_4 = -0.13501102001039084$	$g_4 = -h_3$
$h_5 = -0.085441273882241486$	$g_5 = h_2$
$h_6 = 0.035226291882100656$	$g_6 = -h_1$

After running multiple trials with various sets of control parameters, the original wavelet based nonlinear time-frequency control scheme was modified in attempt to further improve performance. The form of the modified controller is similar to the one designed by Wang and Suh [14] for concurrent speed and position tracking of DC motors. The modified version of the controller implements a proportional controller (P) to compensate the time-delay of the on-line identification process. The gain of the proportional controller was set at 1 for each simulation performed in this study. The output of the proportional control loop is fed into the error signals used by the adaptive algorithms. The overall architecture of the modified controller used to produce the results presented in this research is presented by Figure 6.

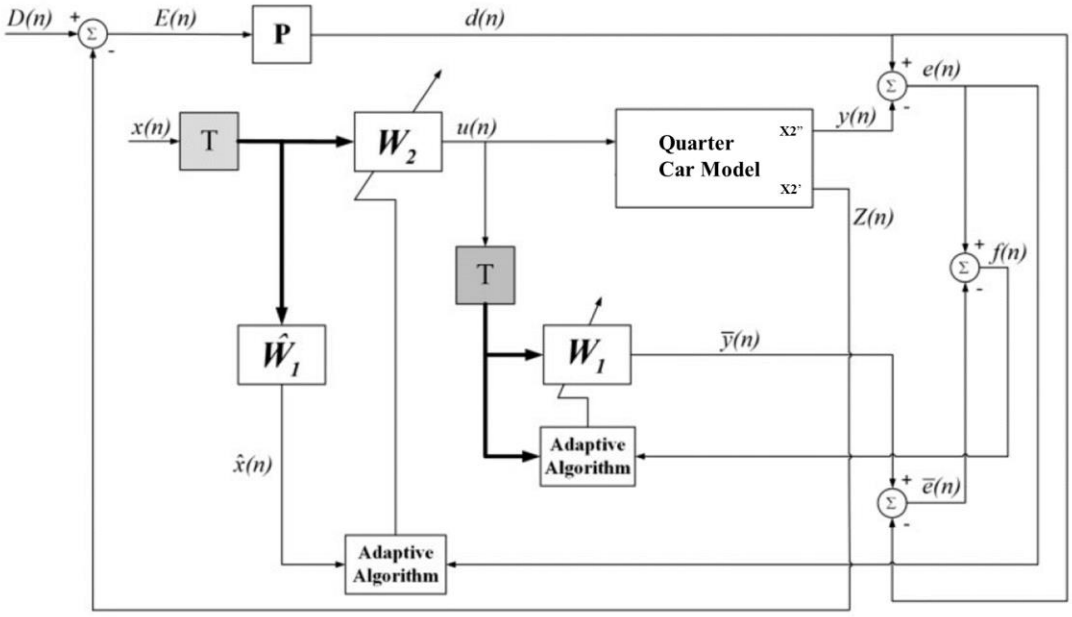

Figure 6: Modified nonlinear time-frequency control with proportional controller

The reference signal provided to the adaptive algorithm for minimizing error is the vertical acceleration of the car body. By minimizing vertical acceleration, forces transferred to the passenger are also minimized. The vertical velocity of the car body is fed into the proportional control loop to create a time varying reference signal to aid in effectively minimizing the vertical displacements of the vehicle. The secondary control parameter for the proportional control loop was chosen as car body velocity because it is the time derivative of the displacement and allows the controller to better predict and compensate for the direction in which the displacement is changing. The combination of these separate control loops creates a way to simultaneously provide vibration and acceleration reduction experienced by the passengers.

3. CAR AND MAGNETORHEOLOGICAL DAMPER MODELS

The models representing the physical systems analyzed in this research will be presented in this section. The nonlinear system used in the simulations consists of a quarter car dynamic model and the modified Bouc-Wen MR damper model.

3.1 Quarter Car Model

A diagram of the quarter car model used in the simulations is show below in Figure 7. This simplified two degree of freedom model accounts for the vertical motion of the wheel and vehicle body. Parameters included by the simplified model are mass, stiffness, and damping coefficient of the wheel and tire, sprung mass, spring stiffness, and the MR damper. The values for these parameters are given in Table 2. To expand this model to the full car representation, pitch, roll, and yaw motions of the vehicle must be related between each quarter car model.

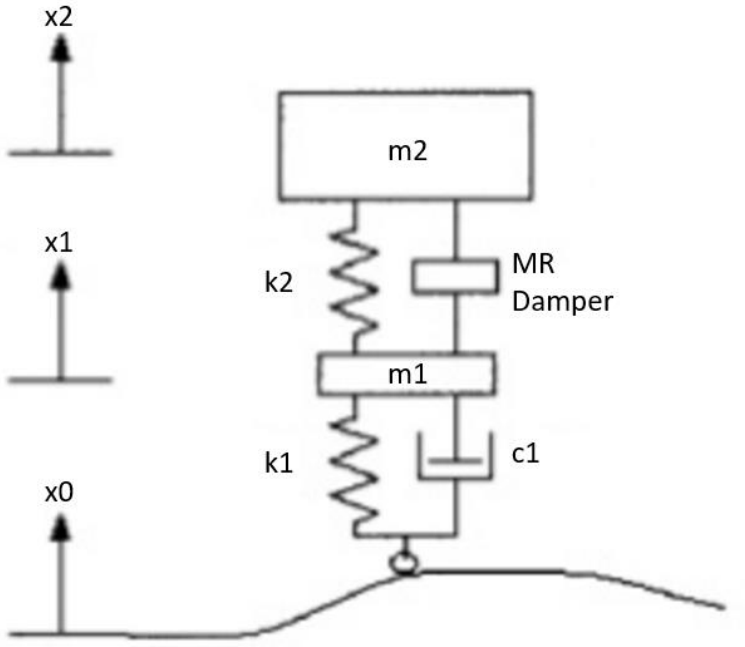

Figure 7: Quarter Car Model

Table 2: Vehicle Parameters

Symbol	Description	Value
m1	Wheel/tire mass	36 kg
m2	Car body mass	240 kg
k1	Wheel/tire stiffness	160000 N/m
k2	Suspension spring stiffness	16000 N/m
c1	Wheel/tire damping coefficient	980 N*s/m

Figure 31 in the Appendix shows the Simulink block diagram of the quarter car model. The governing dynamic equations for the quarter car model, given by Equations 10 and 11, can be expressed as:

$$m_1\ddot{x}_1 = -c_1(\dot{x}_1 - \dot{x}_0) + k_2(x_2 - x_1) - k_1(x_1 - x_0) + F_{MR} \quad [10]$$

$$m_2\ddot{x}_2 = -k_2(x_2 - x_1) - F_{MR} \quad [11]$$

3.2 Modified Bouc-Wen Model

The modified Bouc-Wen model, proposed by Spencer, Dyke *et al*. is implemented in the following simulations and has been widely used to describe the highly nonlinear properties of MR dampers. The model is a set of differential equations describing the hysteretic characteristics of the damper force/velocity response. A diagram identifying the parameters of the modified Bouc-Wen model is given by Figure 8. Experimental verification of the accuracy of the modified Bouc-Wen model performed by Spencer, Dyke et al. is presented in Figure 9 [15].

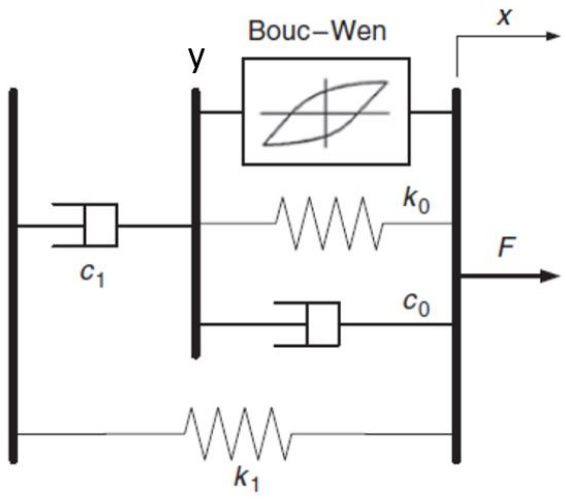

Figure 8: Modified Bouc-Wen Model

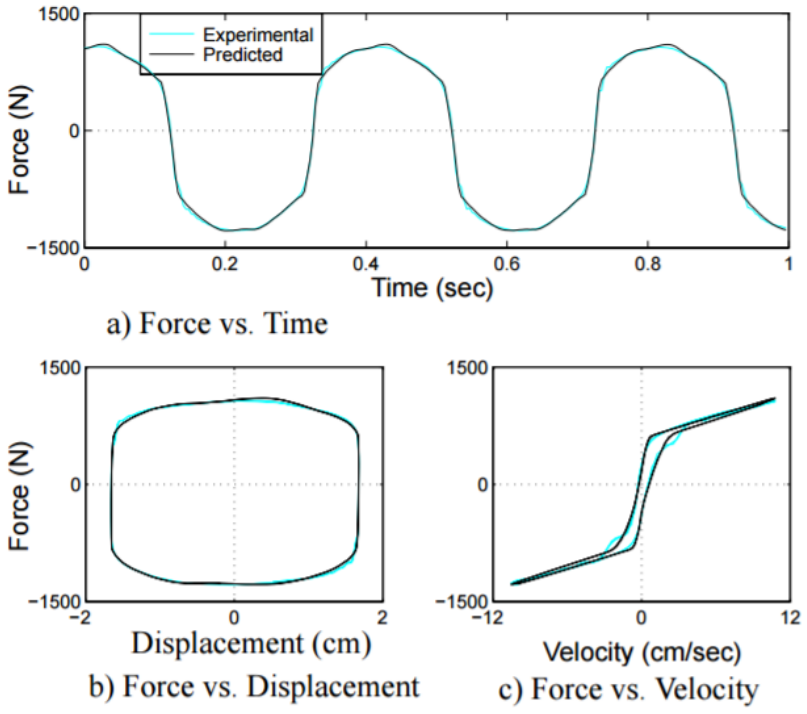

Figure 9: Comparison between the predicted and experimentally obtained responses for the Modified Bouc-Wen Model [15]

Equations 12 - 14 below provide the differential equations associated with the hysteric characteristics of the damper force and velocity response. The force generated by the MR damper is given by Equation 12. The internal velocity of the MR damper, $\dot{y}$ is defined by Equation 13. Z is and evolutionary variable that defines the hysteretic properties of the damper. The shape and size of the hysteretic loop is determined by the parameters δ, γ, and β. The remaining terms in the model are as follows: c_0 is the viscous damping at high velocity, c_1 is the viscous damping at low velocity, k_0 is the stiffness at high velocity, k_1 is the accumulator stiffness, and x_0 is the initial spring displacement. [7]

$$F_{MR} = c_1\dot{y} + k_1(x - x_0) \quad [12]$$

$$\dot{y} = \frac{1}{c_1 + c_0}[\alpha z + c_0\dot{x} + k_0(x - y) \quad [13]$$

$$\dot{z} = -\gamma z|\dot{x} - \dot{y}||z|^{n-1} - \beta(\dot{x} - \dot{y})|z|^n - \delta(\dot{x} - \dot{y}) \quad [14]$$

The terms α, c_0, and c_1, defined by Equations 15, 16, and 17 respectively, are all functions of the electrical current applied to the damper, u. Typical operating ranges for MR dampers in vehicle suspensions are 0 – 1 A or 0 – 1.33 A. The current range selected for this model is 0 – 1 A. The time-delay required for the MR fluid to reach rheological equilibrium is modeled by the first-order filter in Equation 18.

$$\alpha = \alpha(u) = \alpha_a + \alpha_b u \quad [15]$$

$$c_0 = c_0(u) = c_{0a} + c_{0b} u \quad [16]$$

$$c_1 = c_1(u) = c_{1a} + c_{1b} u \quad [17]$$

$$\dot{u} = -\eta(u - v) \quad [18]$$

The values for the modified Bouc-Wen model parameters are given in Table 3 below. A Simulink block diagram of the model is presented in Figure 32.

Table 3: Modified Bouc-Wen parameters

Symbol	Value	Symbol	Value
c_{0a}	784 N*s/m	k_0	3610 N/m
c_{0b}	1803 N*s/ V*m	k_1	840 N/m
c_{1a}	14649 N*s/m	β	2059020 m^{-2}
c_{1b}	34622 N*s/V*m	δ	58
α_a	12441 N/m	γ	136320 m^{-2}
α_b	38430 N/V*m	n	2
x_0	0.0245 m	η	190 s^{-1}

4. METHOD OF EVALUATION

The feasibility of the proposed nonlinear time-frequency controller is evaluated by comparing its performance with the skyhook controller and passive suspension. The performance of each controller is based on its ability to reduce vibration amplitudes and car body acceleration. It is a priority that acceleration of the car body is minimized because this directly translates into the forces transmitted to the passenger. Different test cases for road profile input used in this evaluation are also presented in this section.

4.1 Skyhook Controller

The skyhook control algorithm has been widely applied to control MR dampers in vehicle suspensions with success. Because of its popularity, this control method will be used as the baseline for performance evaluation of the proposed nonlinear time-frequency controller.

The two input parameters needed for the skyhook method are absolute and relative velocities of the sprung mass in the vertical direction. In practical implementation, these values are typically acquired using sensors to record acceleration and relative displacement measurements, then converting these signals to velocities [16]. The velocities $\dot{x}_1$ and $\dot{x}_2$ defined in the quarter car model are used in Equation 19 to construct the skyhook algorithm.

$$F_{skyhook} = \begin{cases} F_{max}, & \dot{x}_2(\dot{x}_2 - \dot{x}_1) > 0 \\ F_{min}, & \dot{x}_2(\dot{x}_2 - \dot{x}_1) < 0 \end{cases} \quad [19]$$

The control force F_{max} is achieved when the applied current is at the maximum value. Likewise, F_{min} is achieved when the current equals zero. A Simulink model of the skyhook controller is presented in the Appendix by Figure 34.

4.2 Passive Vehicle Suspension

The passive vehicle suspension will be compared with the two control schemes previously described. The passive system utilizes the same quarter car model and MR damper as the simulations performed for each control scheme. However, in this case no current is applied to the damper. This provides comparison to the worst case scenario should the control system fail.

4.3 Road Profile Inputs

4.3.1 Multiple Frequency Input

The first test case is given below by Figure 10. This signal is composed by summing three sinusoidal terms at different frequencies (2, 4, and 6 Hz) and will simulate a nonlinear rough road condition. This case evaluates the controller's ability to handle a broadband input signal applied to the physical model.

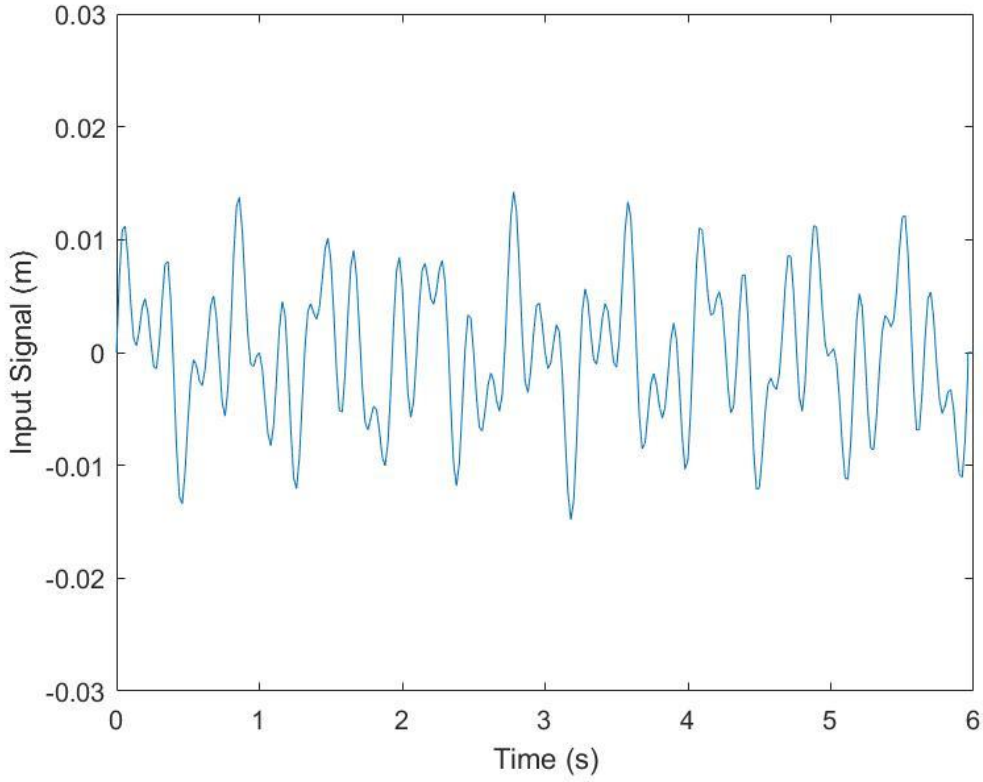

Figure 10: Multiple frequency input test case

4.3.2 Time-Varying Frequency Input

The next test case, given by Figure 11, is a time-varying frequency input signal. Three different frequencies at 2, 4, and 6 Hz are applied to the system successively. This scenario tests the adaptability of the controller and evaluates the controller's performance as frequency is varied.

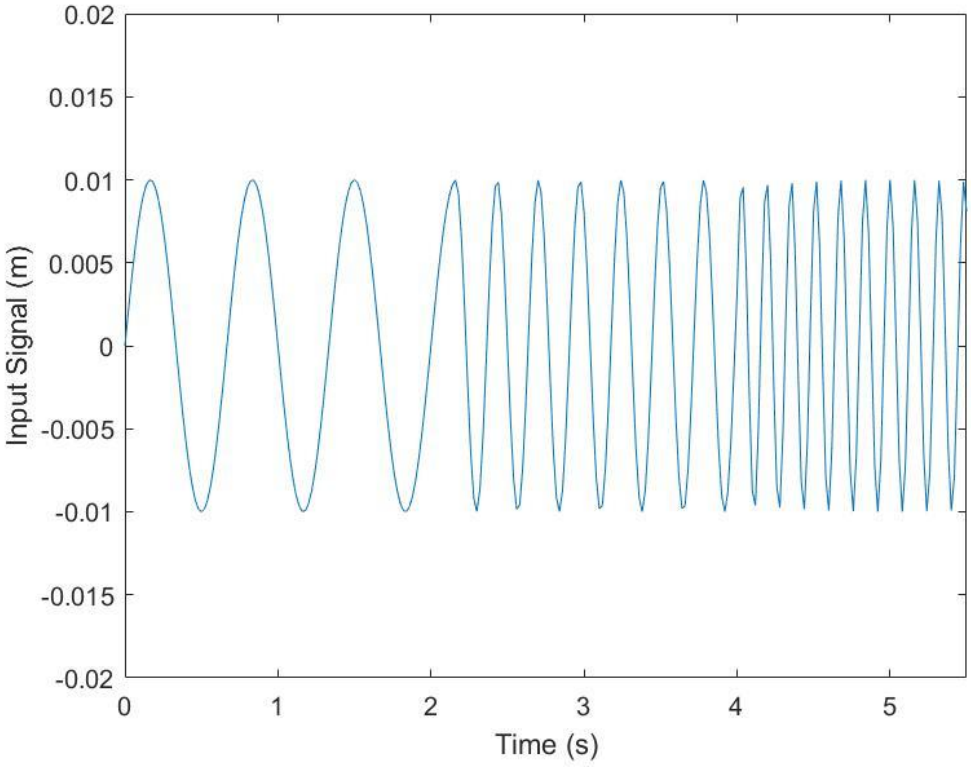

Figure 11: Time varying frequency input test case

4.3.3 Single Bump Input

The final test case shown in Figure 12 simulates the vehicle encountering a large bump in the road profile. This case will determine if the controller is able to react quickly to sudden, large perturbations. Large single bumps or holes in the road profile are the road conditions which are mostly noticeable by the driver and passengers [5]. It is expected that this case will provide the greatest challenge for the proposed nonlinear time-frequency controller because it does not include past information that can be used

to predict the upcoming road condition. The only way to accurately identify a single bump is to use profile scanning sensors to create a preview signal.

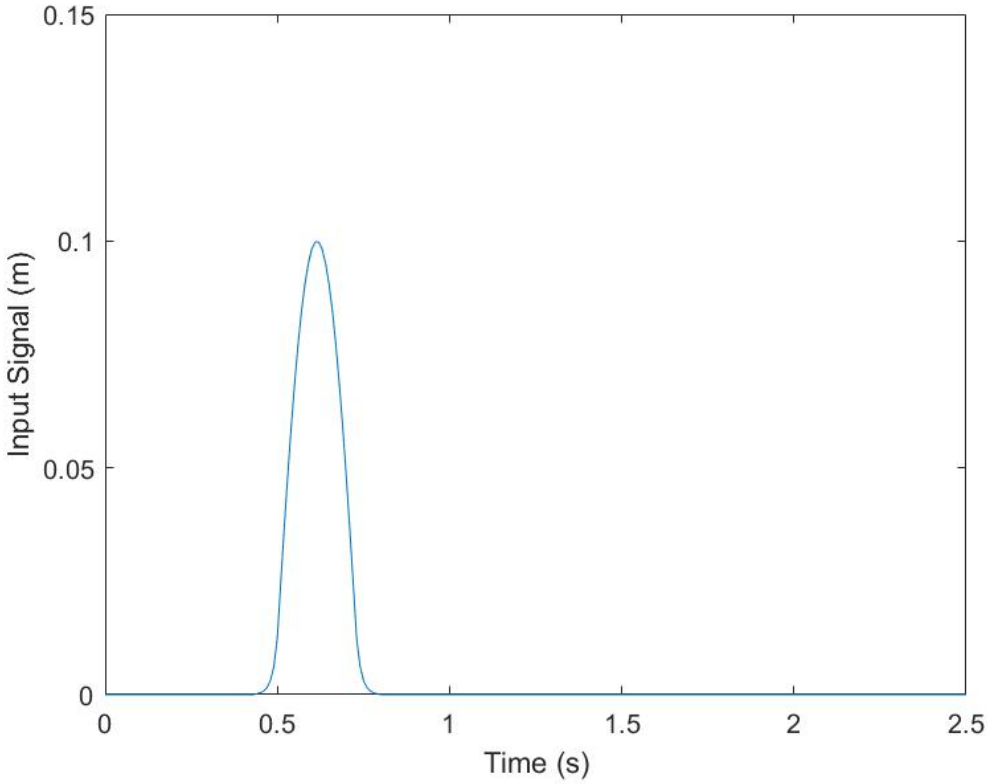

Figure 12: Single bump excitation test case

5. MODELLING RESULTS AND DISCUSSION

This section contains the results of the controller simulations performed for each test case described in the previous section. The results include simulations for the skyhook controller and the proposed Nonlinear Time-Frequency Controller (NTFC) along with comparisons to the passive damping system in which no control is applied. The following plots describe the vertical motion of the car body in terms of absolute displacement and acceleration. Plots of the current applied by the controller and equivalent current simulating rheological equilibrium are included to demonstrate the energy efficiency of each controller.

5.1 Road Excitation with Multiple Frequencies

5.1.1 Skyhook Results

The results of the skyhook control algorithm for the vertical motion of the car body are presented by Figure 13. The skyhook method works well in this case for reducing the amplitude of vibration seen by the car body. It should be noted that there are some spikes in the acceleration plot. Spikes in acceleration are caused when excessive current is applied to the damper at inappropriate times. This presents an issue with the skyhook method because maximum and minimum amounts of applied current are at set values.

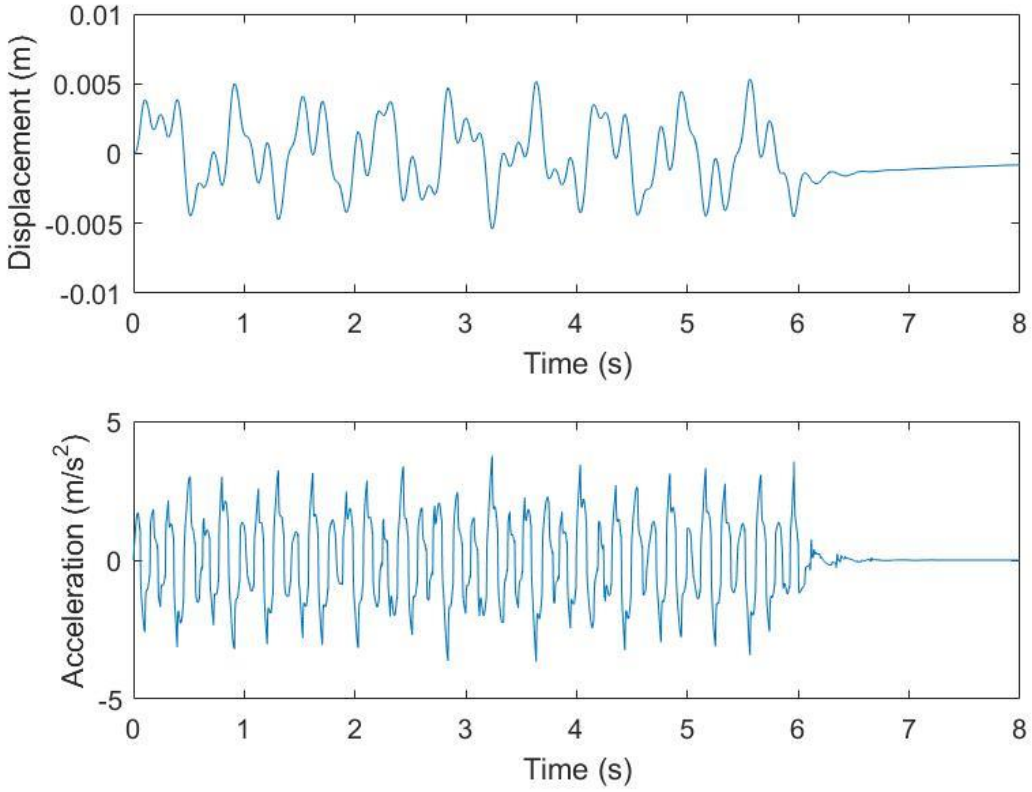

Figure 13: Skyhook results for multiple frequency input

Figure 14 shows the current applied to the MR damper by the skyhook controller. Close inspection and comparison of these plots shows how the time-delay of reaching rheological equilibrium affects the response of the damper. At very high frequencies the time delay is too prominent to allow the full desired current value to be applied.

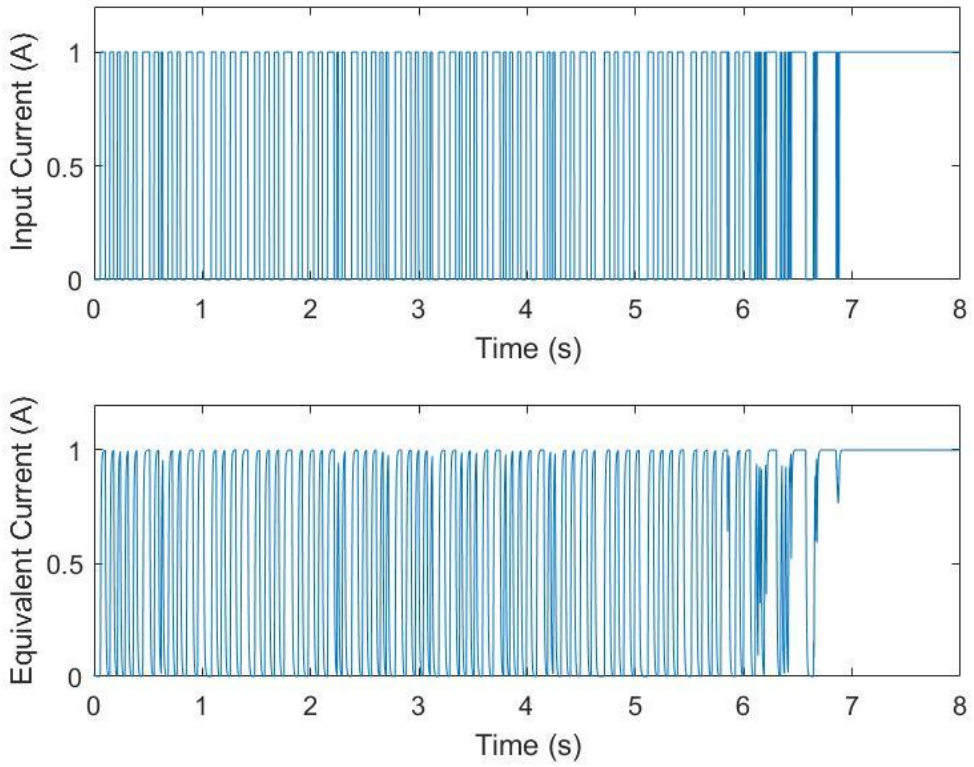

Figure 14: Skyhook controlled current for multiple frequency input

5.1.2 Nonlinear Time-Frequency Control Results

The controller parameters selected for this simulation are given by Table 4 below. The optimization step size μ_2 is much larger than the step size μ_1 (used for system identification) to allow the controller to react more quickly to the error signal.

Table 4: NTFC parameters for multiple frequency excitation

Parameter	Description	Value
dt	Time step (s)	0.0001
N	Wavelet Filter length	128
μ_1	Filter step size	0.0000001
μ_2	Filter step size	0.0002
W1start	Filter initial value	1
W2start	Filter initial value	1

The results of the NTFC for the vertical motion of the car body are presented in Figure 15. The amplitude of vibrations is significantly reduced. The plot of acceleration shows control without excessive spiking.

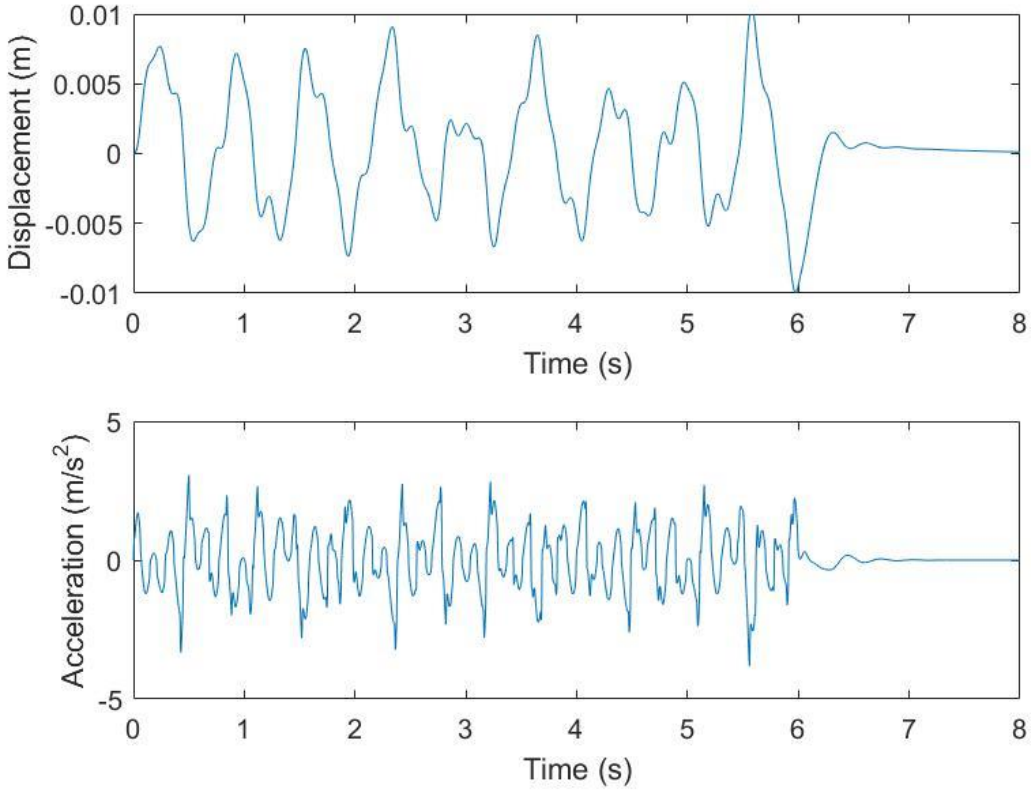

Figure 15: NTFC results for multiple frequency input

The current applied to the MR damper by the nonlinear time frequency controlled is given in Figure 16. The frequency that the current is applied by this controller is much lower than the skyhook controller.

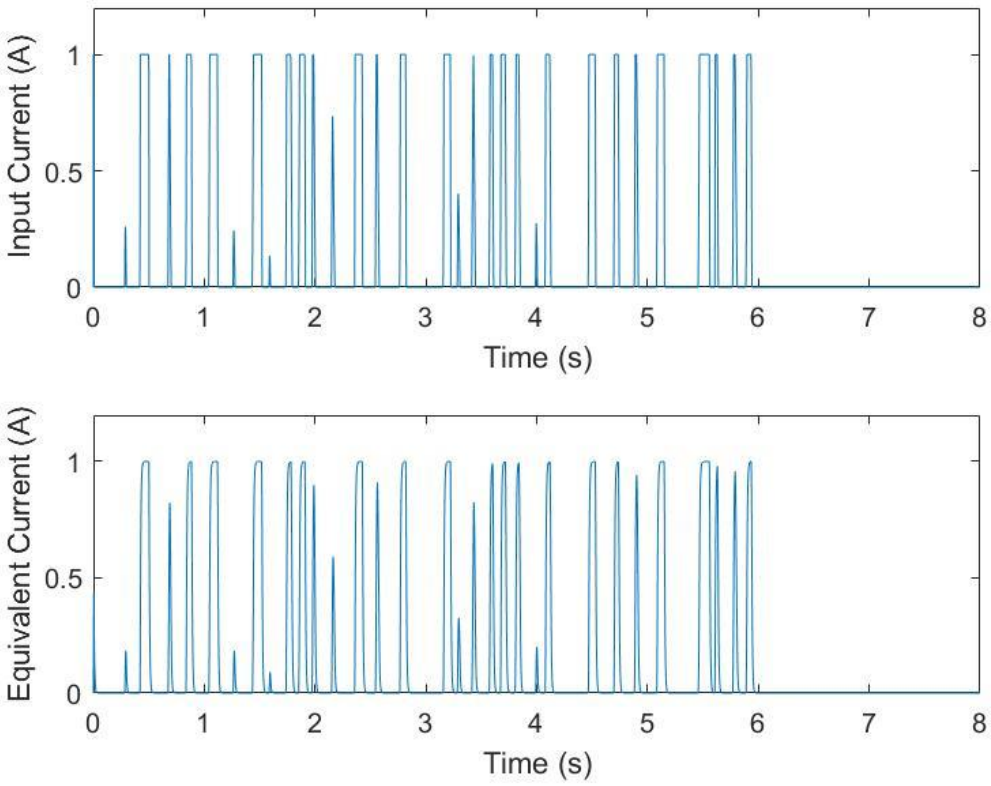

Figure 16: NTFC controlled current for multiple frequency input

Figure 17 and Figure 18 below give the combined plots of skyhook, nonlinear time-frequency, and passive control for the displacement and acceleration of the car body. Both controllers show the ability to significantly reduce the amplitude of vibration compared to the passive system. However, the skyhook controller outperforms the nonlinear time-frequency controller in terms of vibration amplitude.

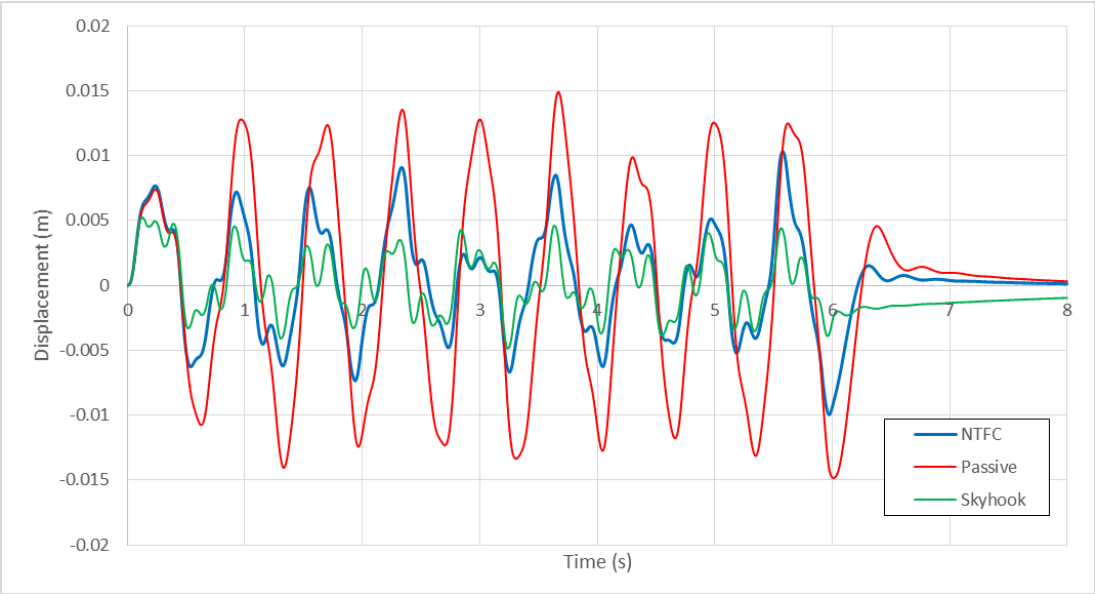

Figure 17: Displacement comparison for multiple frequency input

From Figure 18, it can be concluded that the nonlinear time-frequency controller provided a better response than the skyhook controller in minimizing acceleration of the car body. The results of the skyhook controller show more frequent and greater magnitude spikes in acceleration. Overall, the acceleration response of the passive system is considered acceptable. However, the large magnitude of displacement amplitude makes it undesirable.

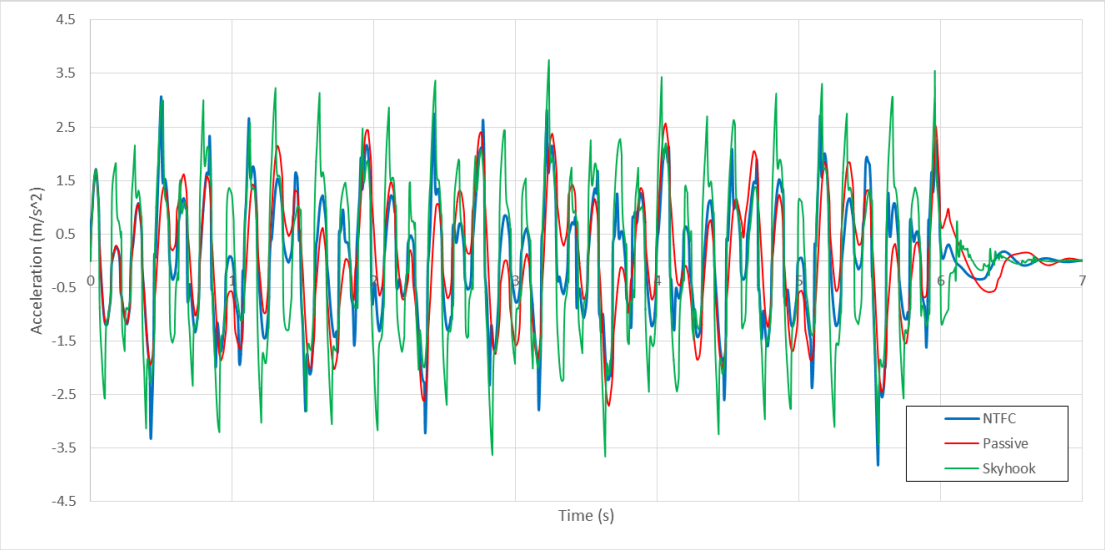

Figure 18: Acceleration comparison for multiple frequency input

5.2 Road Excitation with Time-Varying Frequencies

5.2.1 Skyhook Results

The skyhook control results are shown in Figure 19 and Figure 20. The controller is able to successfully provide a reduction in vibration amplitude. As the higher frequency excitations are applied, the amplitude of displacement decreases. The acceleration response becomes worse at higher frequencies.

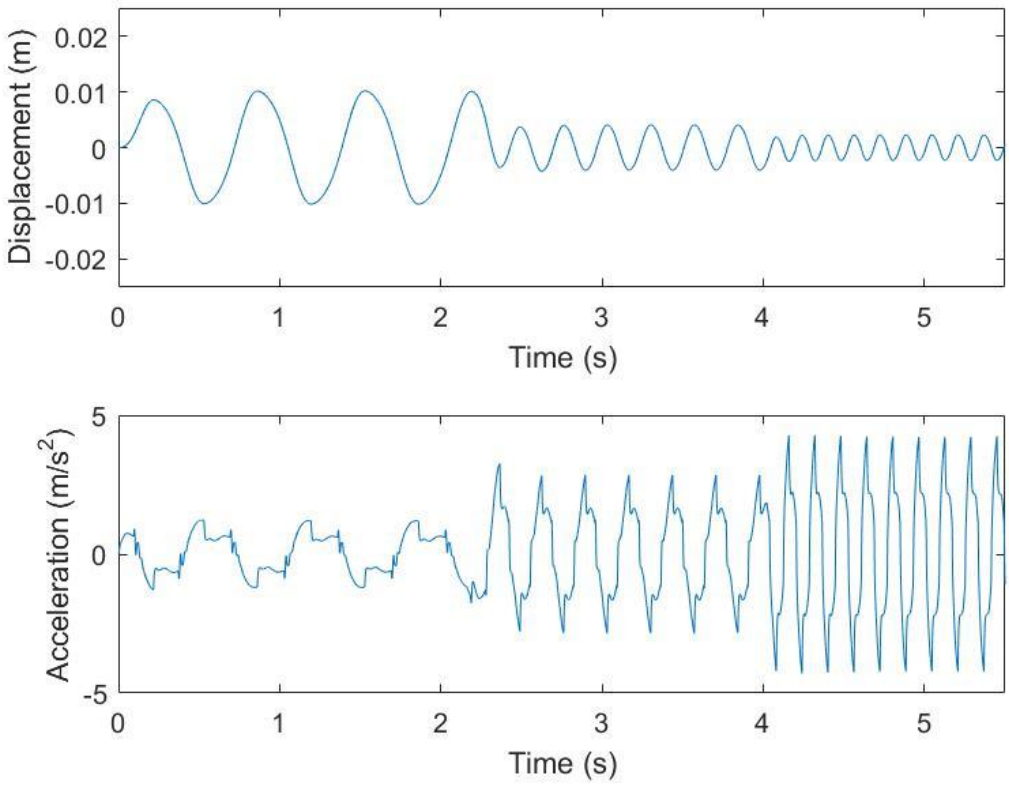

Figure 19: Skyhook results for time-varying frequency input

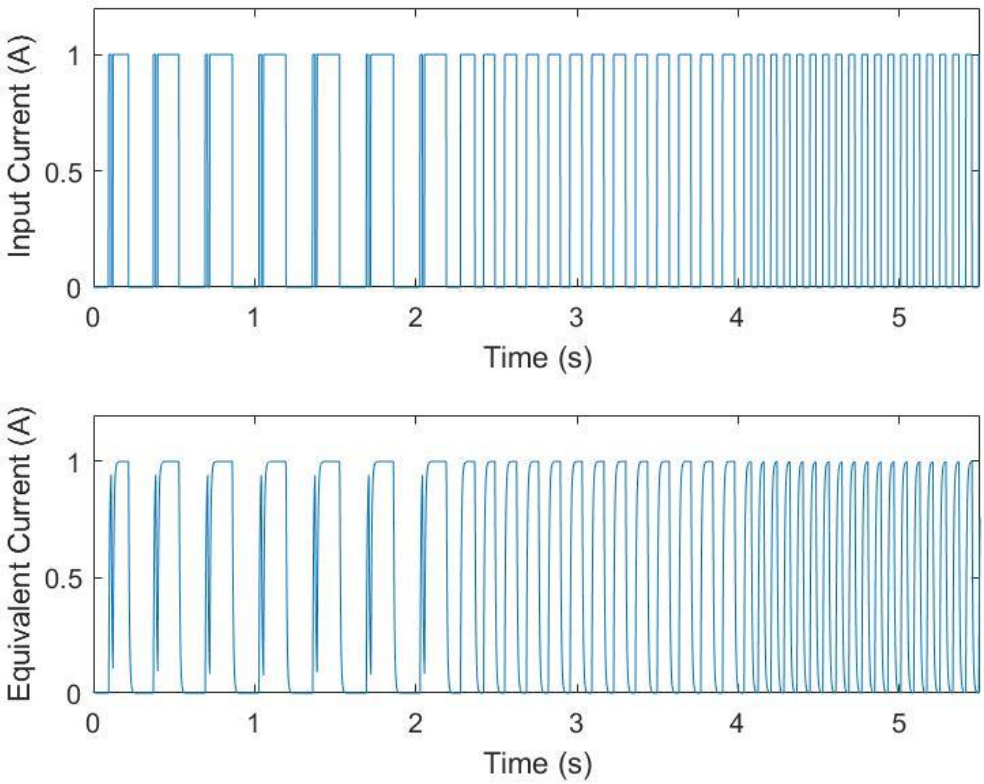

Figure 20: Skyhook controlled current for time-varying frequency input

5.2.2 Nonlinear Time-Frequency Control Results

The controller parameters for this test case are the same as those listed in Table 4 for the case of multiple frequency input. Figure 21 provides the simulation results for the nonlinear time-frequency controller. The results show that the controller is able to provide a good reduction in vibration amplitude while also keeping acceleration minimized over a range of applied frequencies.

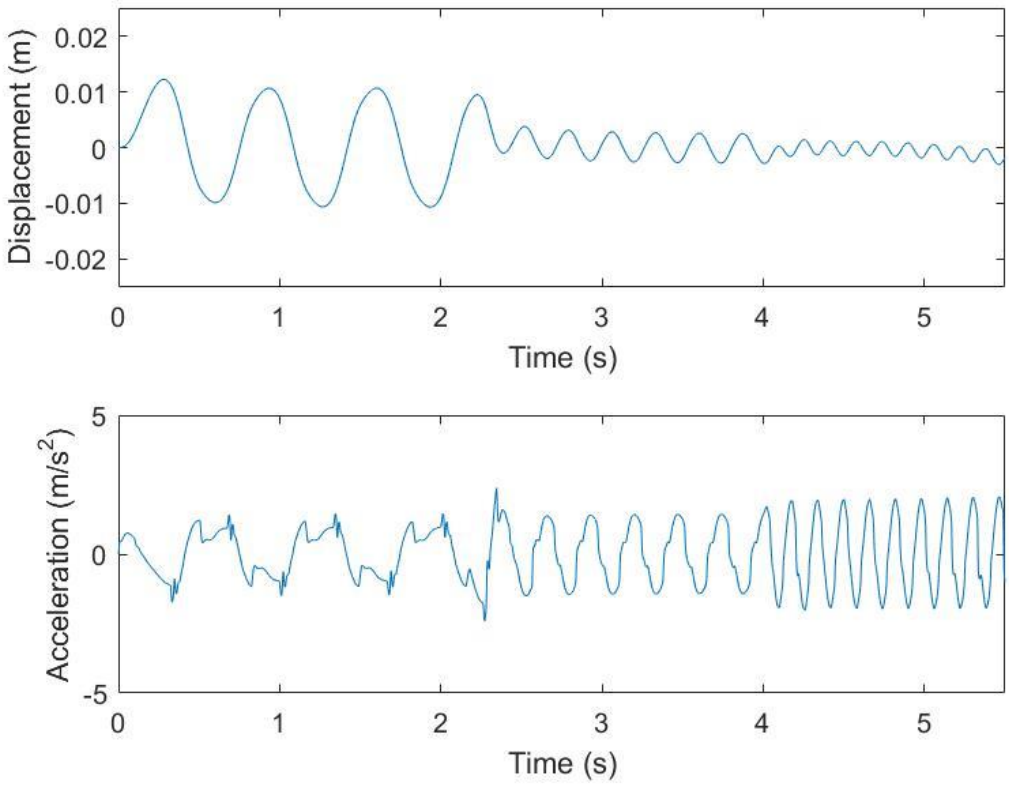

Figure 21: NTFC results for time-varying frequency input

Figure 22 shows how the controller adapts to a varying input and modulates the applied current to optimize the response. The nonlinear time-frequency control method is able to provide a significantly improved response while using less power than the skyhook controller.

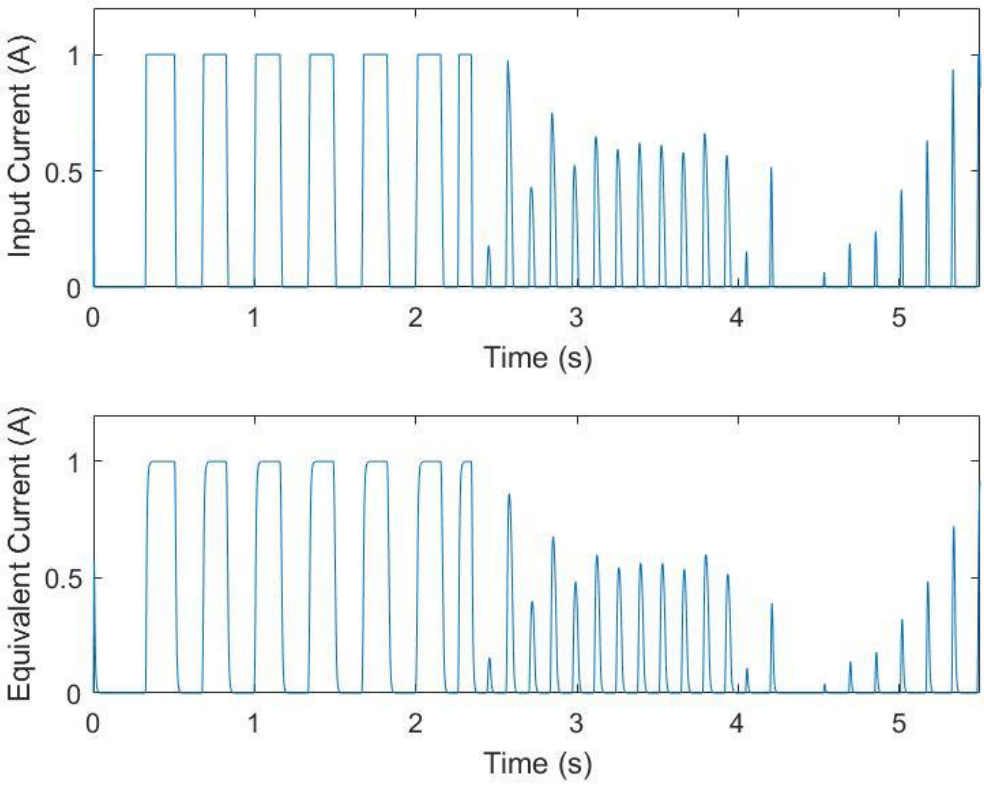

Figure 22: NTFC controlled current for time-varying frequency input

The combined displacement response for each controller is provided in Figure 23 for a clear comparison. Both controllers showed vast improvement over the passive system; specifically at the lowest applied frequency. At higher frequencies, the nonlinear time-frequency controller produced the best response in terms of displacement amplitude.

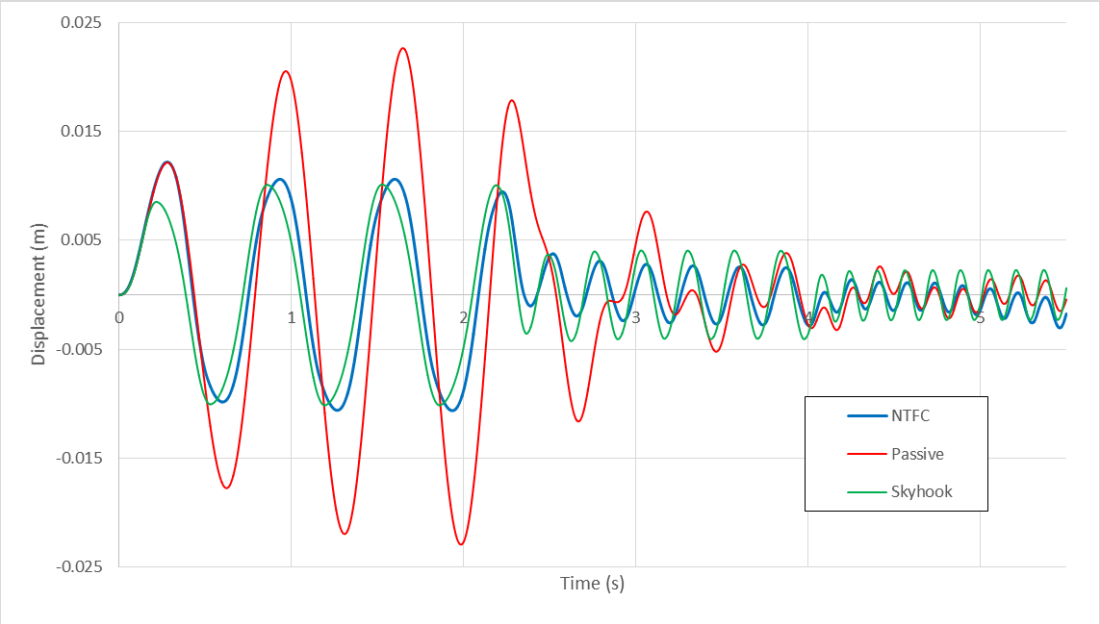

Figure 23: Displacement comparison for time-varying frequency input

The acceleration response for each controller is shown in Figure 24. At the lowest applied frequency, the skyhook and nonlinear time-frequency controllers both yield smaller magnitude acceleration than the passive system. However, at the highest frequency considered, the skyhook controller performs poorly and shows many large spikes in acceleration.

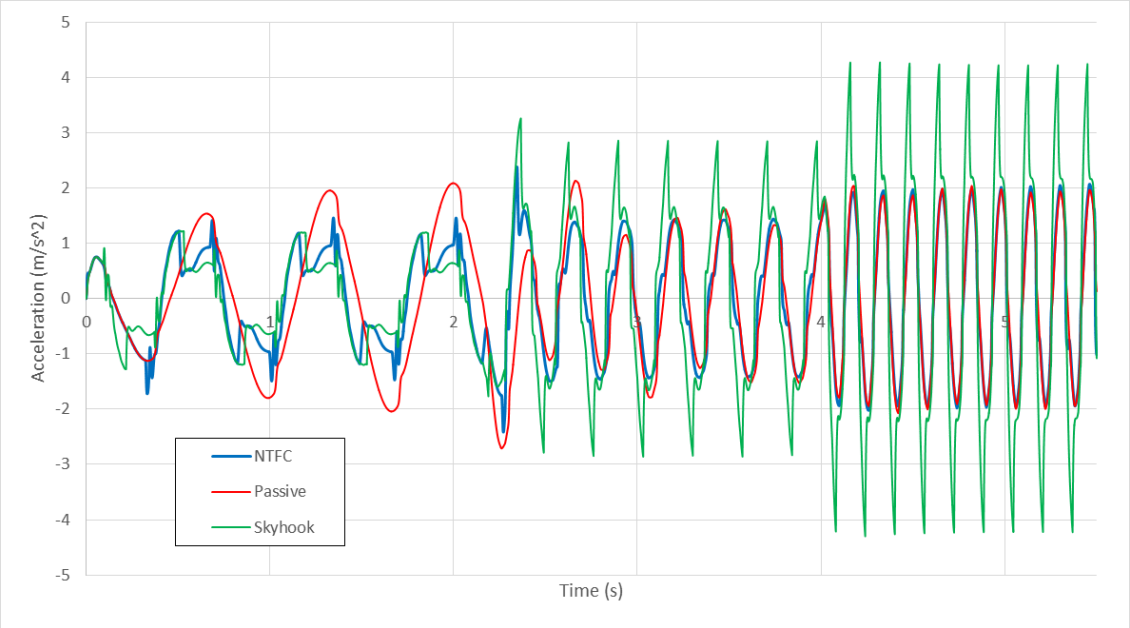

Figure 24: Acceleration comparison for time-varying frequency input

5.3 Large Bump Excitation

5.3.1 Skyhook Results

Figure 25 below show the results of the skyhook controller in response to a sudden bump excitation. The plot shows a good reduction in displacement and fast return to equilibrium with minimal oscillation. The small oscillations after the bump can be considered negligible. However, this causes fluctuations in the controlled current that are unnecessary and inefficient. The plots for current applied during this simulation are shown in Figure 26.

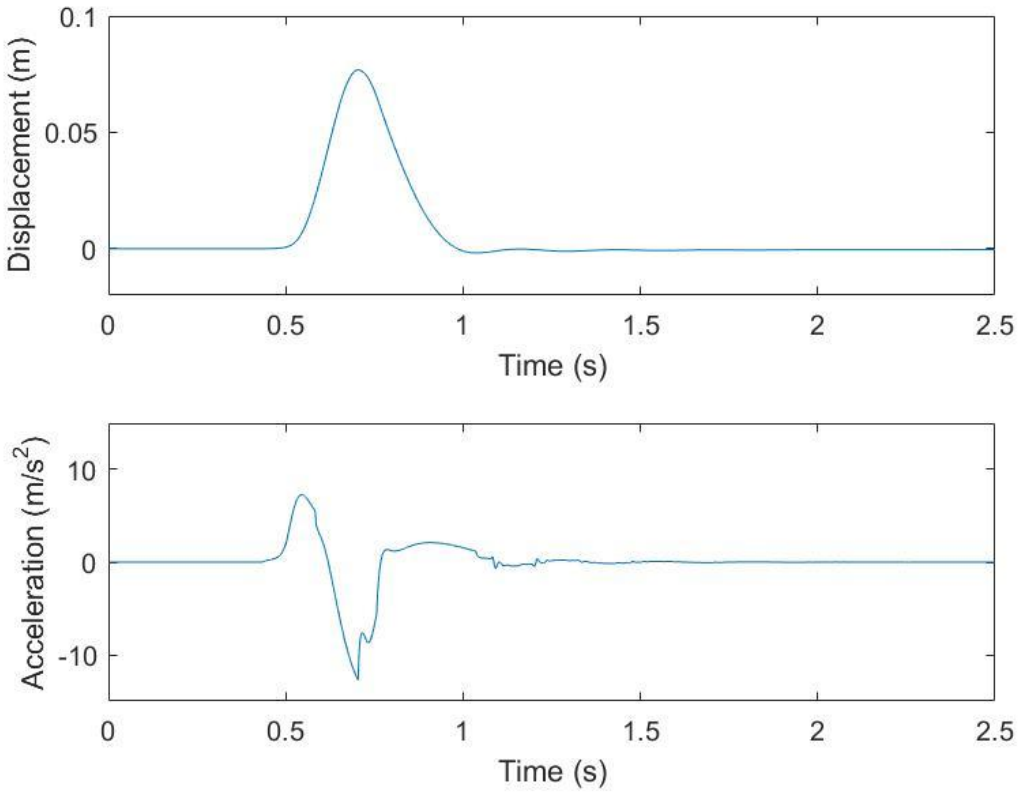

Figure 25: Skyhook results for bump excitation

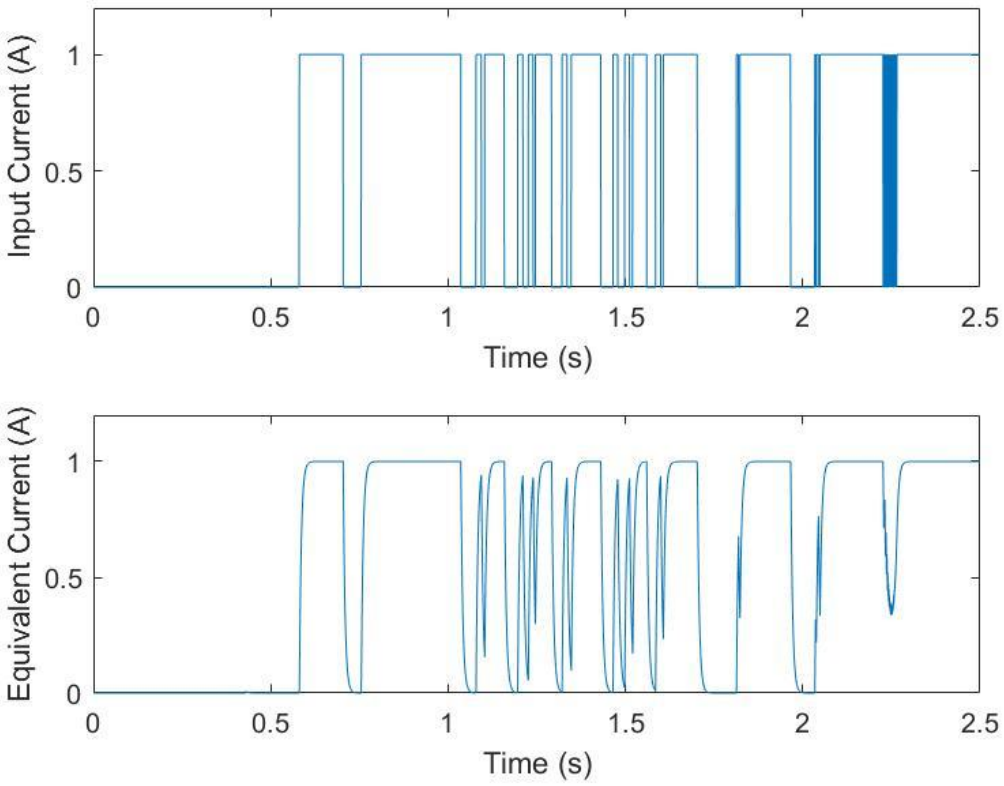

Figure 26: Skyhook controlled current for bump excitation

5.3.2 Nonlinear Time-Frequency Control Results

The controller parameters for the case of large bump excitation are listed in Table 5. The only parameter different from the previous test cases is the regression step size μ_2. This parameter is altered to provide the most improved response.

Table 5: NTFC Parameters for bump excitation

Parameter	Description	Value
dt	Time step (s)	0.0001
N	Wavelet Filter length	128
μ_1	Filter step size	0.0000001
μ_2	Filter step size	0.00001
W1start	Filter initial value	1
W2start	Filter initial value	1

The vehicle response for the simulation using the nonlinear time-frequency control method is provided in Figure 27. The controller provides a reduction in displacement amplitude with negligible oscillations. The current applied by the controller is efficient and without fluctuation. The issue with this controller is that the starting current value is based on the initial value of the filters and is set at 1 amp before the controller reacts to a perturbation in the input signal. For ideal vibration amplitude reduction in this case, the current must be zero as the vehicle approaches the bump and compresses the damper. The plots of current are shown in Figure 28.

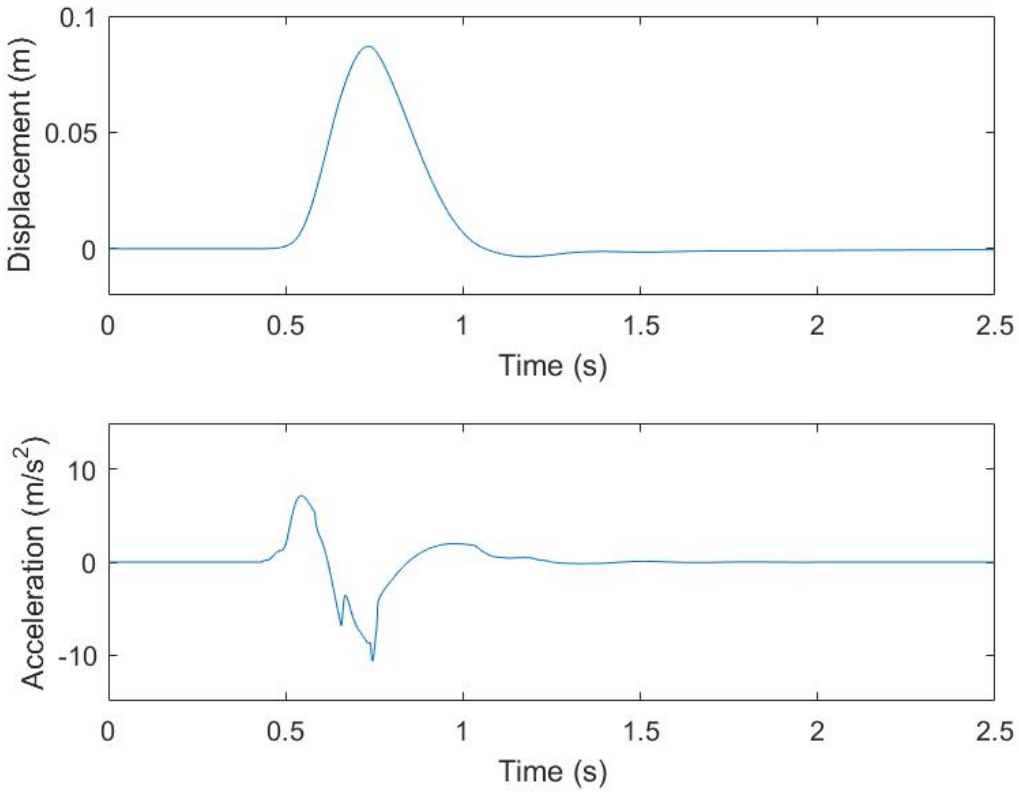

Figure 27: NTFC results for bump excitation

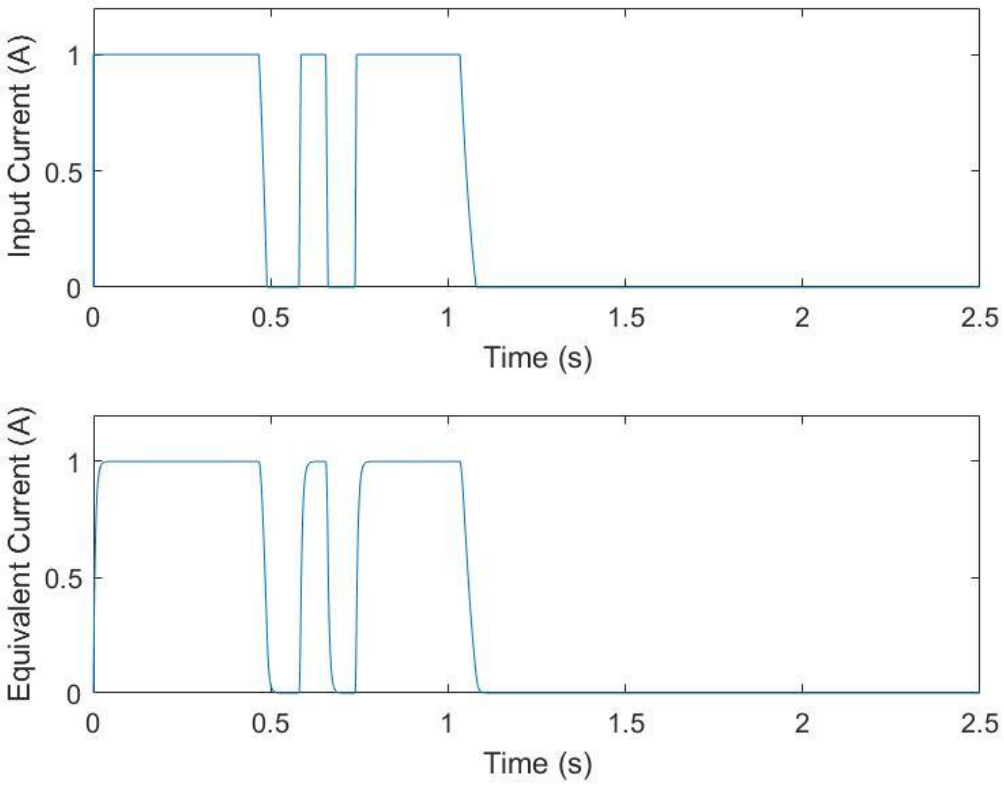

Figure 28: NTFC controlled current for bump excitation

The displacement responses of the controllers are compared in Figure 29. The passive suspension performs very poorly without control and shows large displacement amplitude with oscillations. Both the NTFC and skyhook controllers are able to dissipate the energy of the bump excitation with negligible oscillation. However, the skyhook controller provides a better response than NTFC in terms of displacement amplitude. The skyhook controller response is also able to bring the car body mass back to its equilibrium position more quickly than the NTFC.

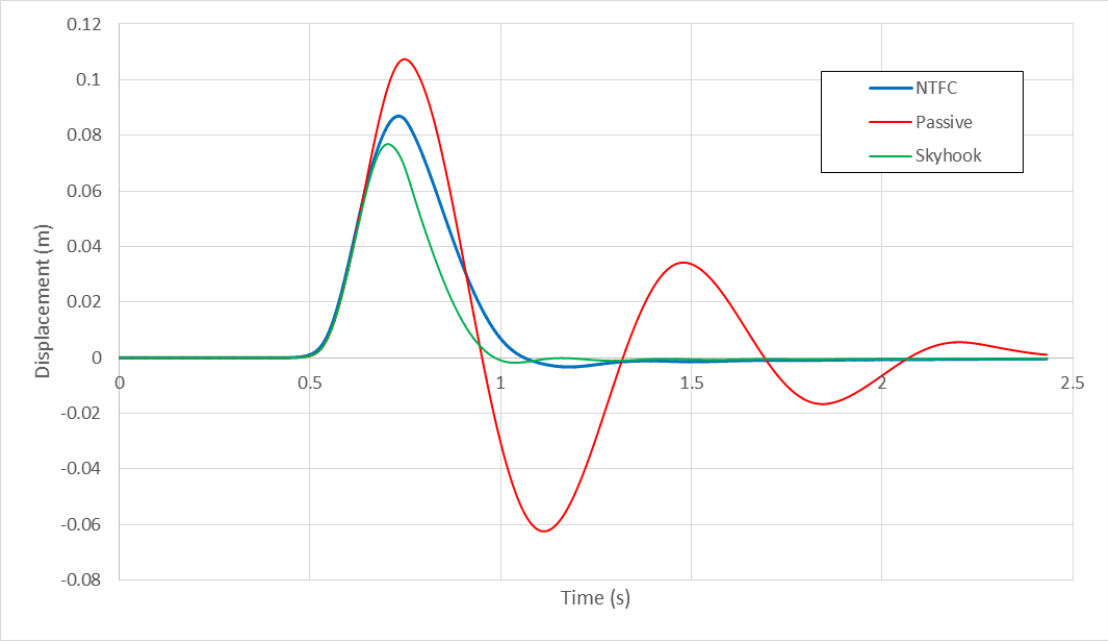

Figure 29: Displacement comparison for bump excitation

Figure 30 provides the comparison of the acceleration responses for each controller. The passive system continues to have large magnitude accelerations after the bump due to oscillations. The controllers are both able to minimize the acceleration after the bump. However, the nonlinear time-frequency controller is able to provide the lowest acceleration magnitudes. The responses of the passive system and skyhook controller from 1 – 1.5 seconds both show sudden reverses in acceleration whereas the NTFC controller does not.

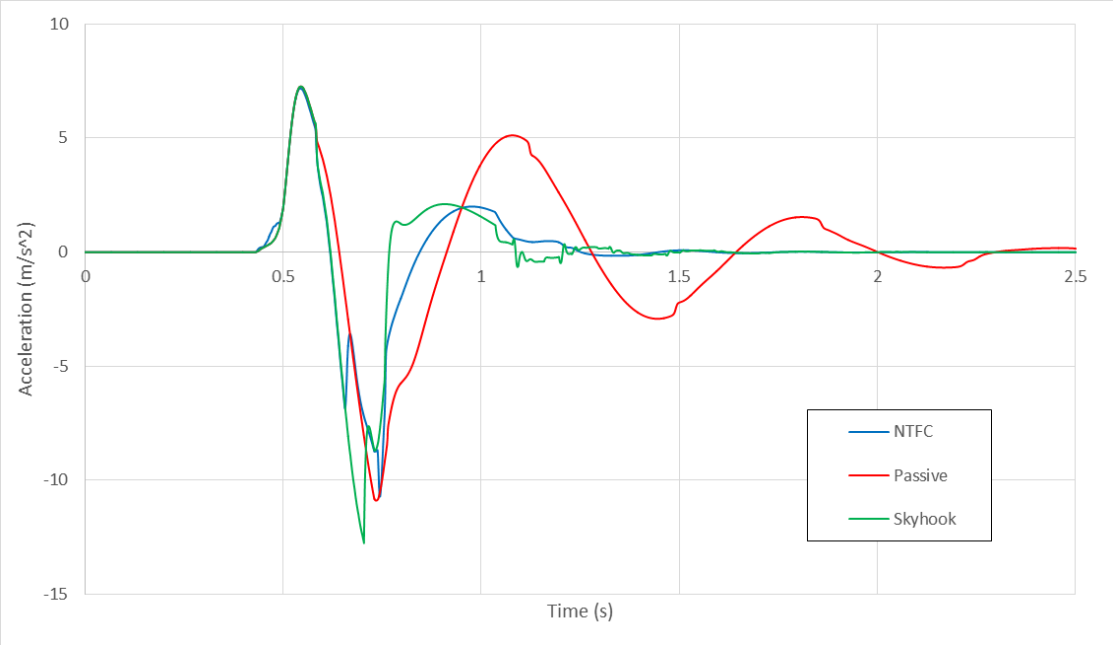

Figure 30: Acceleration comparison for bump excitation

5.4 Discussion of Performance

The results of the simulations performed show that the proposed nonlinear time-frequency controller is capable of reducing the amplitude of vibrations and acceleration experienced by the car body. The adaptive nature of the controller is displayed by the reduction of acceleration throughout changes in excitation frequencies. The proposed nonlinear time-frequency controller outperformed the skyhook algorithm greatly at high frequencies. The skyhook controller performs well for cases where the reduction of vibration amplitude is given preference to minimizing acceleration. However, the absolute displacement of the car body is not as important to ride quality as vertical acceleration and forces transmitted to the passenger.

The difference in power efficiency between the two controllers becomes more apparent as frequency is increased. The controlled current from the proposed NTFC controller shows much less fluctuation than the skyhook controller. The high spikes in acceleration from the skyhook simulations are mostly due to the maximum current value being applied at times that are not ideal. Residual current due to the time-delay also creates high damping forces that are detrimental to the response after the desired current returns to the minimum value. A significant disadvantage of the skyhook controller is that the applied current is at a set value; whereas the nonlinear time-frequency controller can better modulate the applied current between the maximum and minimum values. It is possible that different current operating ranges will produce better results. In order to best compare the performance of the controllers, current ranges were kept the same. The cut-off of the maximum current value likely hinders the performance of the NTFC controller. The results presented in this research support the fulfillment of the objective to design an improved controller for MR dampers in vehicle suspension.

6. CONCLUSIONS

The proposed nonlinear time-frequency control method evaluated in this research can be successfully applied to MR dampers in vehicle suspension to reduce vibration amplitudes and forces transmitted to the passenger. For every test case presented, the nonlinear time-frequency control outperformed the skyhook control algorithm in terms of minimizing acceleration of the car body. If the priority of the controller is only to reduce the amplitude of vibrations, the skyhook controller should be selected over the proposed nonlinear time-frequency controller. Because nonlinear time-frequency control is a feed-forward controller, it has a better ability to compensate for the time delay of the MR damper compared to a feed-back controller such as skyhook. Another benefit of the nonlinear time-frequency controller is that it is adaptive. This is important so that the controller can account for changes in the physical model. The adaptive algorithm also benefits the system because when the controller is implemented in a physical system, additional nonlinearities not previously accounted for in simulation can be managed. For example, depending on how the vehicle is loaded, the mass values will be different and the controller must be able to adapt to provide an ideal response.

Due to the highly nonlinear nature of MR dampers, the NTFC controller showed sensitivity to controller parameters. Selection of the filter length N and step sizes μ_1 and μ_2 are critical to the success of the controller. Unfortunately, these parameters must often be determined by trial and error. The test cases of sinusoidal input and large bump excitation performed in this research required different regression step sizes in the feed-

forward loop to be used in order to provide the best response. In a real world scenario, numerous physical tests must be performed so that the controller parameters can be optimized to provide improved performance in every case.

7. FUTURE WORK

Before actual implementation in a vehicle, the controller should be tested in simulations using half-car and full-car models. These models present added challenges in accounting for roll, pitch, and yaw of the vehicle body. It is likely that additional controllers will be needed to relate the motions of each corner of the vehicle to the individual MR dampers.

Once simulations have been performed to show that the controller is compatible with the full car model, actual implementation should be tested. Difficulties may arise in creating repeatable system inputs on an actual road for testing controller parameters. The parameters will need to be selected based on the expected road conditions. For example, off-road conditions will likely have higher amplitude and lower frequency vibrations compared to street or track cases.

REFERENCES

[1] S. M. Savaresi, C. Poussot-Vassal, C. Spelta, O. Sename, and L. Dugard. Semiactive suspension control design for vehicles. Butterworth-Heinemann, Elsevier, 2006.

[2] S. H. Zareh, F. Matbou, and A. A. A. Khayyat, "Experiment of new laboratory prototyped magneto-rheological dampers on a light commercial vehicle using neuro-fuzzy algorithm," *Journal of Vibration and Control*, pp. 3007–3019, 2014.

[3] D. Q. Truong and K. K. Ahn, "MR Fluid Damper and Its Application to Force Sensorless Damping Control System," *Smart Actuation and Sensing Systems - Recent Advances and Future Challenges*, 2012.

[4] "Magnetic Damper - Magnetorheological Damper," *Magnetic Damper*. http://www.formula1-dictionary.net/damper_magnetorheological.html

[5] P. Krauze, J. Kasprzyk, Vibration control in quarter-car model with magnetorheological dampers using FxLMS algorithm with preview, 13th European Control Conference ECC 2014, Strasbourg, France, June 24-27, 2014.

[6] Using Nonlinear Kalman Filtering to Estimate Signals. (n.d.). Retrieved February 17, 2017, from http://academic.csuohio.edu/simond/pubs/ESDNonlinear.pdf

[7] Amini, F., Hazaveh, N., & Rad, A. (2013). Wavelet PSO-Based LQR Algorithm for Optimal Structural Control Using Active Tuned Mass Dampers. *Computer-Aided Civil and Infrastructure Engineering,* 542-557.

[8] Pohoryles, D. A., & Duffour, P. (2013). Adaptive control of structures under dynamic excitation using magnetorheological dampers: an improved clipped-optimal control algorithm. *Journal of Vibration and Control,21*(13), 2569-2582. doi:10.1177/1077546313510543

[9] Choi, S., Li, W., Yu, M., Du, H., Fu, J., & Do, P. X. (2016). State of the art of control schemes for smart systems featuring magneto-rheological materials. *Smart Materials and Structures, 25*(4), 043001. doi:10.1088/0964-1726/25/4/04300

[10] Yan, G., & Zhou, L. L. (2006). Integrated fuzzy logic and genetic algorithms for multi-objective control of structures using MR dampers. *Journal of Sound and Vibration,296*(1-2), 368-382. doi:10.1016/j.jsv.2006.03.011

[11] Suh, C., & Liu, M. (n.d.). "*Control of cutting vibration and machining instability: A time-frequency approach for precision, micro and nano machining*," John Wiley & Sons, 2013.

[12] Lewallen, Colby Foster (2016). Novel Active Magnetic Bearing Control for a High-Speed Flywheel. Master's thesis, Texas A & M University. Available electronically from http : / /hdl.handle .net /1969 .1 /158082.

[13] Liu, M., & Suh, C. S. (2015). Active Magnetic Bearings for High Speed Spindle Design With Nonlinear Time-Frequency Control. Volume 4B: Dynamics, Vibration, and Control. doi:10.1115/imece2015-50994

[14] Wang, X., & Suh, C. S. (2016). Precision concurrent speed and position tracking of brushed dc motors using nonlinear time-frequency control. Journal of Vibration and Control.

[15] Spencer, B. F., Dyke, S. J., Sain, M. K., & Carlson, J. D. (1997). Phenomenological Model for Magnetorheological Dampers. Journal of Engineering Mechanics,123(3), 230-238.

[16] Song, X. (2009). Cost-Effective Skyhook Control for Semiactive Vehicle Suspension Applications. *The Open Mechanical Engineering Journal*, *3*(1), 17-25.

APPENDIX

Simulink Models

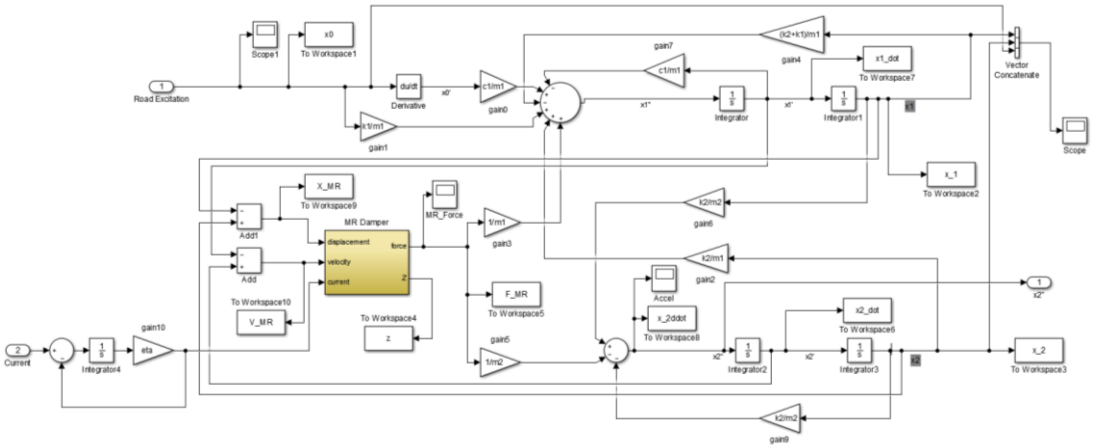

Figure 31: 2 DOF Quarter Car Simulink Model

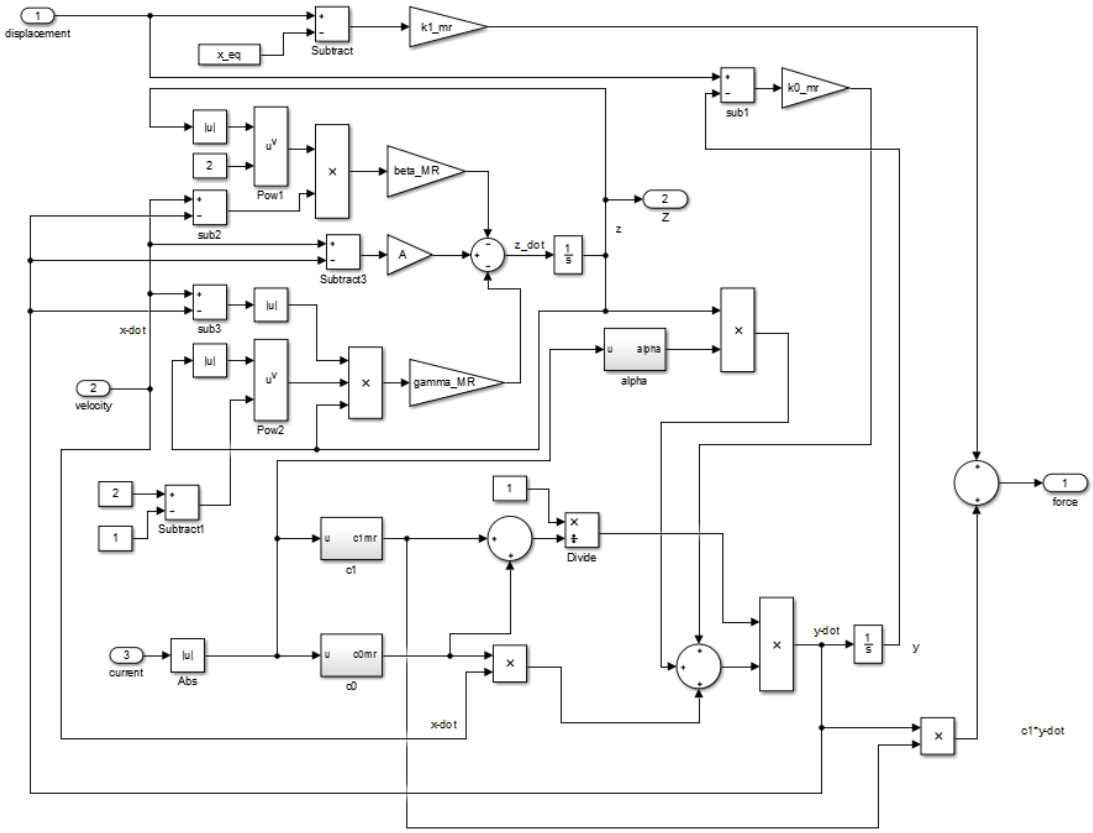

Figure 32: Modified Bouc-Wen Simulink Model

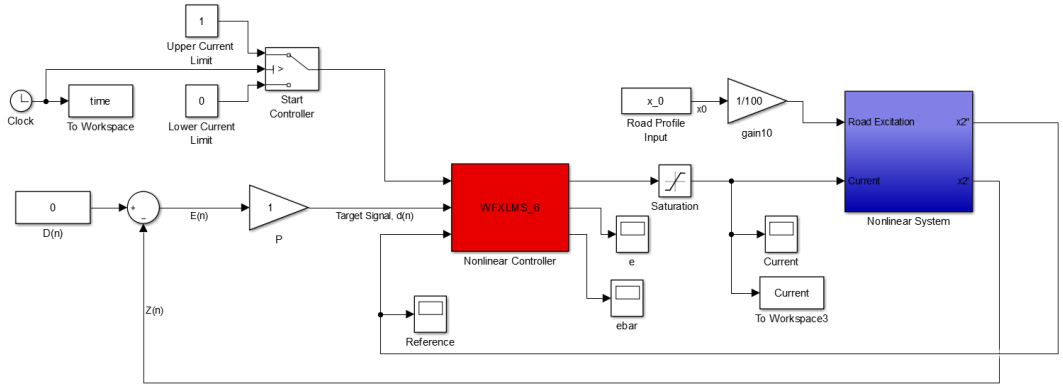

Figure 33: NTFC Controller Configuration

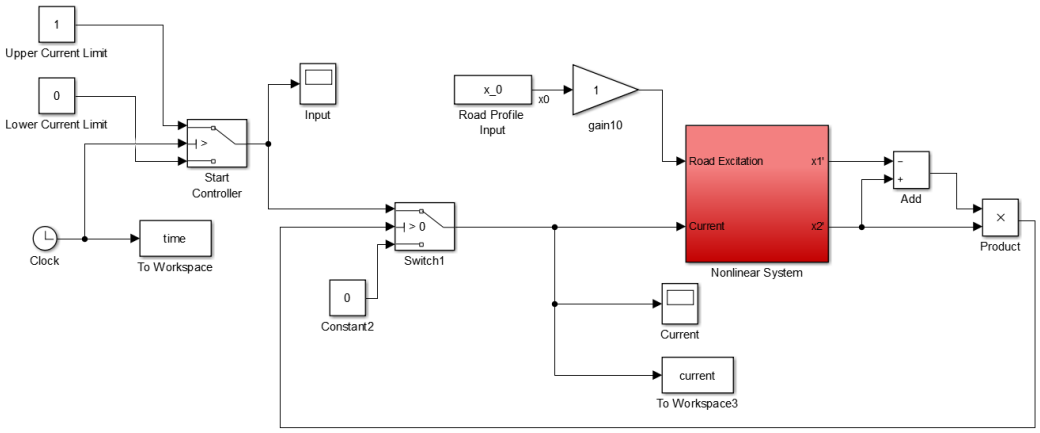

Figure 34: Skyhook Controller Configuration